



Article

First Characterization of *Ostreopsis* cf. *ovata* (Dinophyceae) and Detection of Ovatoxins during a Multispecific and Toxic *Ostreopsis* Bloom on French Atlantic Coast

Nicolas Chomérat ^{1,*}, Elvire Antajan ², Isabelle Auby ², Gwenael Bilien ¹, Liliane Carpentier ³, Marie-Noëlle de Casamajor ⁴, Florian Ganthy ², Fabienne Hervé ³, Magali Labadie ⁵, Claire Méteigner ², Camille Paradis ⁵, Myriam Perrière-Rumèbe ², Florence Sanchez ⁴, Véronique Séchet ³ and Zouher Amzil ^{3,*}

¹ Ifremer, LITTORAL, 29900 Concarneau, France; gwenael.bilien@ifremer.fr

² Ifremer, LITTORAL, 33120 Arcachon, France; elvire.antajan@ifremer.fr (E.A.); isabelle.auby@ifremer.fr (I.A.); florian.ganthy@ifremer.fr (F.G.); claire.meteigner@ifremer.fr (C.M.); myriam.rumebe@ifremer.fr (M.P.-R.)

³ Ifremer, PHYTOX, 44000 Nantes, France; liliane.carpentier@ifremer.fr (L.C.); fabienne.herve@ifremer.fr (F.H.); veronique.sechet@ifremer.fr (V.S.)

⁴ Ifremer, LITTORAL, 64600 Anglet, France; marie.noelle.de.casamajor@ifremer.fr (M.-N.d.C.); florence.sanchez@ifremer.fr (F.S.)

⁵ Centre Anti-Poison et Toxicovigilance, CHU de Bordeaux, 33076 Bordeaux, France; magali.labadie@chu-bordeaux.fr (M.L.); camille.paradis@chu-bordeaux.fr (C.P.)

* Correspondence: nicolas.chomerat@ifremer.fr (N.C.); zouher.amzil@ifremer.fr (Z.A.); Tel.: +33-2-98-10-42-80 (N.C.); +33-2-40-37-40-69 (Z.A.)



Citation: Chomérat, N.; Antajan, E.; Auby, I.; Bilien, G.; Carpentier, L.; Casamajor, M.-N.d.; Ganthy, F.; Hervé, F.; Labadie, M.; Méteigner, C.; et al. First Characterization of *Ostreopsis* cf. *ovata* (Dinophyceae) and Detection of Ovatoxins during a Multispecific and Toxic *Ostreopsis* Bloom on French Atlantic Coast. *Mar. Drugs* **2022**, *20*, 461. <https://doi.org/10.3390/md20070461>

Academic Editor: Jordi Molgó

Received: 8 June 2022

Accepted: 10 July 2022

Published: 18 July 2022

Publisher's Note: MDPI stays neutral with regard to jurisdictional claims in published maps and institutional affiliations.



Copyright: © 2022 by the authors. Licensee MDPI, Basel, Switzerland. This article is an open access article distributed under the terms and conditions of the Creative Commons Attribution (CC BY) license (<https://creativecommons.org/licenses/by/4.0/>).

Abstract: Blooms of the benthic toxic dinoflagellate genus *Ostreopsis* have been recorded more frequently during the last two decades, particularly in warm temperate areas such as the Mediterranean Sea. The proliferation of *Ostreopsis* species may cause deleterious effects on ecosystems and can impact human health through skin contact or aerosol inhalation. In the eastern Atlantic Ocean, the toxic *O. cf. ovata* has not yet been reported to the north of Portugal, and the only species present further north was *O. cf. siamensis*, for which the toxic risk is considered low. During summer blooms of unidentified *Ostreopsis* species on the French Basque coast (Atlantic) in 2020 and 2021, people suffered from irritations and respiratory disorders, and the number of analyzed cases reached 674 in 2021. In order to investigate the causes, sampling was carried out during summer 2021 to (i) taxonomically identify *Ostreopsis* species present using a molecular approach, (ii) isolate strains from the bloom and culture them, and (iii) characterize the presence of known toxins which may be involved. For the first time, this study reports the presence of both *O. cf. siamensis* and *O. cf. ovata*, for which the French Basque coast is a new upper distribution limit. Furthermore, the presence of ovatoxins a, b, c, and d in the environmental sample and in a cultivated strain in culture confirmed the toxic nature of the bloom and allowed identifying *O. cf. ovata* as the producer. The present data identify a new health risk in the area and highlight the extended distribution of some harmful dinoflagellates, presumably in relation to climate change.

Keywords: *Ostreopsis* cf. *ovata*; ovatoxins; intoxication; microscopy; phylogeny; LC–MS/MS; human respiratory symptoms

1. Introduction

Primarily considered as a tropical dinoflagellate genus described from the Gulf of Thailand (Siam) [1], *Ostreopsis* has been more frequently reported in warm temperate areas, probably as a consequence of climate change in the past decades [2]. In the Mediterranean Sea, *Ostreopsis* has been mentioned since the 1970s, but it has become increasingly frequent with massive blooms, causing detrimental effects on marine benthic communities [3,4] and on human health through skin contact [5,6], toxic aerosols [7,8], and contaminated seafood [9,10].

To date, 11 species have been described and are taxonomically valid [11], but only two species include a morpho-molecular characterization [12,13]. While genus identification is relatively easy through light microscopy because of its typical teardrop shape, most of the species share rather similar morphological characters including thecal plate organization, and they can hardly be distinguished by light microscopy, especially when they co-occur [14–16]. Furthermore, a high degree of morphological variability exists within a given species, which makes the use of genetic methods essential for reliable identification at species level [17]. Phylogenetic studies inferred from ribosomal genes (domains of the large subunit, LSU) and intergenic transcribed spacers (ITS regions) revealed the existence of at least 13 major clades that could potentially correspond to different species [18–20]; however, to date, some of these genotypes have not yet been taxonomically identified owing to cryptic morphologies or a lack of morphological information [21,22]. Recent studies successfully clarified the taxonomic identity of some of these ribotypes [16,19,20,23], but such approaches are absolutely needed for the remaining genotypes to clarify the complex taxonomy of the genus.

The toxins produced by *Ostreopsis* species are analogues of palytoxin (PLTX), a highly potent marine toxin [24], first isolated from the zoanthid *Palythoa toxica* [25]. PLTX and its analogues may affect human health via ingestion of contaminated seafood, skin contact with seawater, and inhalation of marine aerosols [6,26–29]. Of the 11 taxonomically described species in the genus [11], the species *O. siamensis*, *O. maccarenensis*, *O. cf. ovata*, and *O. farrussoi* produce some of the PLTX analogues (ovatoxins, ostreocins, and maccarenotoxins).

The ovatoxin group (OVTX) includes several analogues of PLTX, named after the organism *Ostreopsis* cf. *ovata* in which they have been primarily identified during toxic blooms in the Mediterranean Sea [30]. On the basis of profiles acquired by liquid chromatography coupled with high-resolution tandem mass spectrometry (LC-HRMS/MS), these compounds were identified as PLTX analogues, with ovatoxin a (OVTX-a), the first for which the structure was elucidated [30–32]. OVTX-a is structurally very similar to PLTX, but lacks two oxygen atoms. Since 2010, other analogues of the OVTX group have been characterized in Mediterranean strains of *O. cf. ovata*: OVTX-b, -c, -d, and -e [33], OVTX-f [34], OVTX-g [35], OVTX-h [36], and OVTX-l [37]. Except for OVTX-a, among these analogues, no complete chemical structure has been elucidated, and only fragmentations by HRMS allowed formulating structural hypotheses. Toxin profiles of Mediterranean strains of *O. cf. ovata* reported so far appear to be dominated by OVTX-a followed by OVTX-b, the isomers OVTX-d and -e, OVTX-c, and isobaric PLTX [37–39]. Other ovatoxins have been identified, e.g., OVTX-i, j1, j2, and k in *O. farrussoi* isolated from Lebanese and Cypriot coasts [13,40]. Mediterranean OVTX isomers (OVTX-a, -b, -d, -e) have been identified in Japanese strains of *Ostreopsis* spp., named OVTX-a AC, -b AC, -d AC, and -e AC [41], as well as OVTX-a IK2, -d IK2, and -e IK2 [42].

In the tropical species *O. siamensis* and *O. maccarenensis*, ostreocins -A, -B, -D, and -E1 (OSTs) [43–47] and maccarenotoxins -a, -b, and -c (McTXs) [46–48] have been identified, respectively.

The majority of *Ostreopsis* poisonings are through inhalation, direct contact leading to skin irritation [6,48–53], or eye contact [52,54]. In temperate areas, toxic blooms accompanied by respiratory problems and skin irritation in humans exposed to marine aerosols containing algal toxins and/or cells debris and seawater [29] have been reported for several areas of the Mediterranean Sea in the two last decades [55]. Among the three species recorded so far in the Mediterranean Sea, *O. cf. ovata*, *O. cf. siamensis* now considered as clearly divergent from *O. siamensis* [18,19], and *O. farrussoi*, the toxic effects have mainly been attributed to *O. cf. ovata*. Intoxication episodes associated with toxic blooms of *O. cf. ovata* occurred during the summer in the northwestern Mediterranean Sea, e.g., on the Italian coast of Genoa in 2005 and 2006 [56], Spanish coast in 2006 [57], and Algerian coast in 2009 [58]. In Genoa, more than 200 people near the beaches felt symptoms during the bloom of *O. cf. ovata* in 2005, among which 20 were hospitalized [56]. On the French Mediterranean coast, 47 intoxications were reported during bloom episodes between 2006

and 2009. The symptoms described correspond to skin irritations induced by direct contact with cells or mucus, along with irritations of the respiratory tract as well as nausea, fever, dizziness, coughing, and headaches induced by aerosols of *O. cf. ovata* [5].

In the western Atlantic Ocean, *Ostreopsis* outbreaks were also reported in western tropical parts of the Brazilian coasts [59–61], where both *O. cf. ovata* and *O. cf. siamensis* were present. In the eastern Atlantic, *Ostreopsis* spp. were detected on the Azores [62], the Canary Islands [59], Morocco [63], and southern Portugal, where *O. cf. siamensis* was first detected in 2008 and even bloomed in 2017 [64,65]. As reported in 2011, *O. cf. siamensis* was also present at several sites of the Cantabrian Sea (northern Spain) since 2007 [66]. While *O. cf. ovata* was later found in samples from Portugal [67–69], it has never been detected in northern places such as the Cantabrian and Basque coasts, where only *O. cf. siamensis* was shown to be present and considered to be the unique *Ostreopsis* species present in this area to date [70,71].

The present study reports atypical *Ostreopsis* bloom events at the end of summer 2020 and mid-summer 2021 on the French Basque coast, causing several health issues to surfers and swimmers, with about 700 people affected in 2021. This work aimed to identify the species present during the bloom using a genetic approach on isolated environmental cells and from cultivated strains, as well as characterize the toxin profile using LC–MS/MS.

2. Results

2.1. Respiratory Disorders and Cutaneous Irritations Observed during Summer Blooms on the French Basque Coast

In 2020, for the first time, a few reports of respiratory symptoms (about 10) were mentioned by swimmers and people frequenting beaches of Hendaye on the French Basque coast (between 4 September and 13 September), and numerous *Ostreopsis* cells were identified on a macroalgal sample collected at Hendaye (Figure 1). Nevertheless, because the number of reported cases remained low, and since it occurred at the end of summer, no further investigations of the origin of this toxicity were conducted. Since *O. cf. siamensis* was known to be recurrently present in the area, these effects were attributed to this species without any complementary analysis.

In 2021, an unusual outbreak of *Ostreopsis* starting in early August on some beaches of the Basque coast (Erromardie and Lafitenia beaches, near Saint-Jean-de-Luz, Figure 1) was associated with health disorders, and a great number of people reported symptoms. From a total of 830 reports of health disorders, after removal of duplicates, 674 cases were verified and confirmed by the Poison Control Center of the university hospital in Bordeaux. Beach users reported various respiratory and cutaneous symptoms (difficulty breathing, irritations, headaches, dry cough, nose irritation, eye irritation and/or dermatitis, and general malaise) after direct contact with water and/or after inhalation of marine aerosols. In addition, metallic taste has also been reported. Several health issues were also mentioned by people who visited beaches of other close localities such as Hendaye and Biarritz (Figure 1). Furthermore, closures of some beaches were decided by local authorities to prevent intoxications. The symptoms disappeared within 2 days without a need to medicate when people moved away from the area concerned by the *Ostreopsis* bloom.

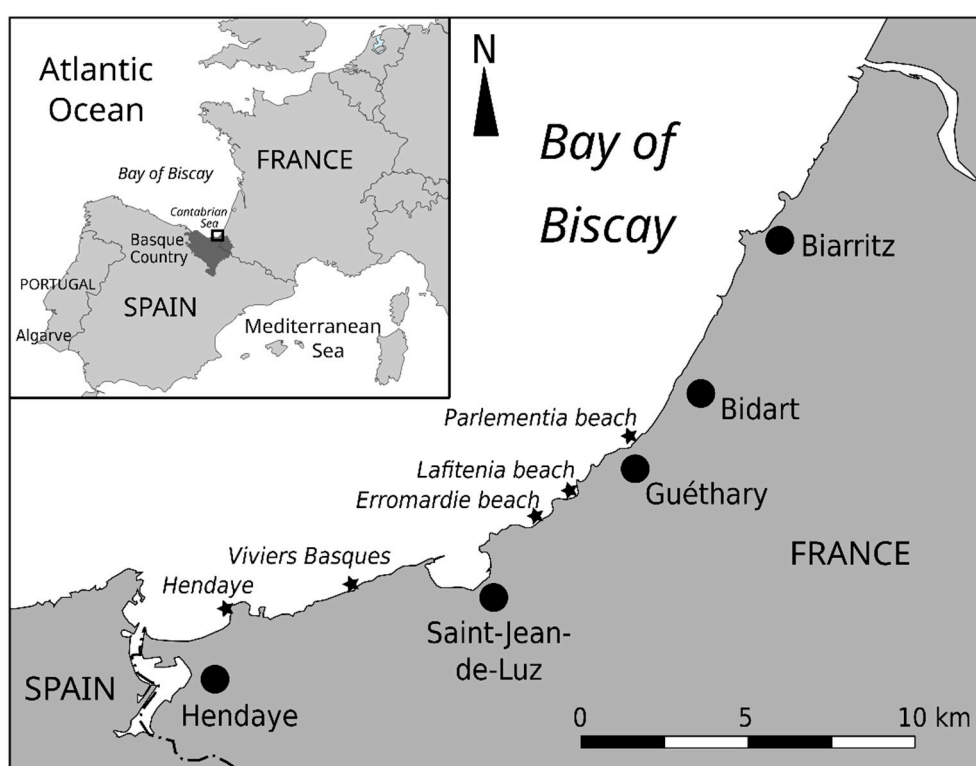


Figure 1. Map showing the location of Basque country and sites on the French Basque coast where proliferations of *Ostreopsis* spp. were observed in summers of 2020 and 2021 (stars).

Because of the importance of the phenomenon and number of affected people in summer 2021, a complete investigation of this toxic event was realized on the basis of regular sampling.

Initial results of *Ostreopsis* cell counts from early August revealed abundances of about 50×10^4 cells·L $^{-1}$ in water samples and 80×10^4 cells·g $^{-1}$ FW of macroalgae (fresh weight *Gelidium corneum*) at Erromardie (Figure 2). In samples collected after 8 August and in September, cell concentrations decreased at the three investigated sites (Figure 2) indicating a decline in the bloom, and abundances were low at the end of September. During September, at some other localities (Guétary and Biarritz), visible aggregates containing high cell concentrations of cells were occasionally observed forming a scum-like accumulation on the surface of the water in areas containing macroalgae or rocks (Figure 3).

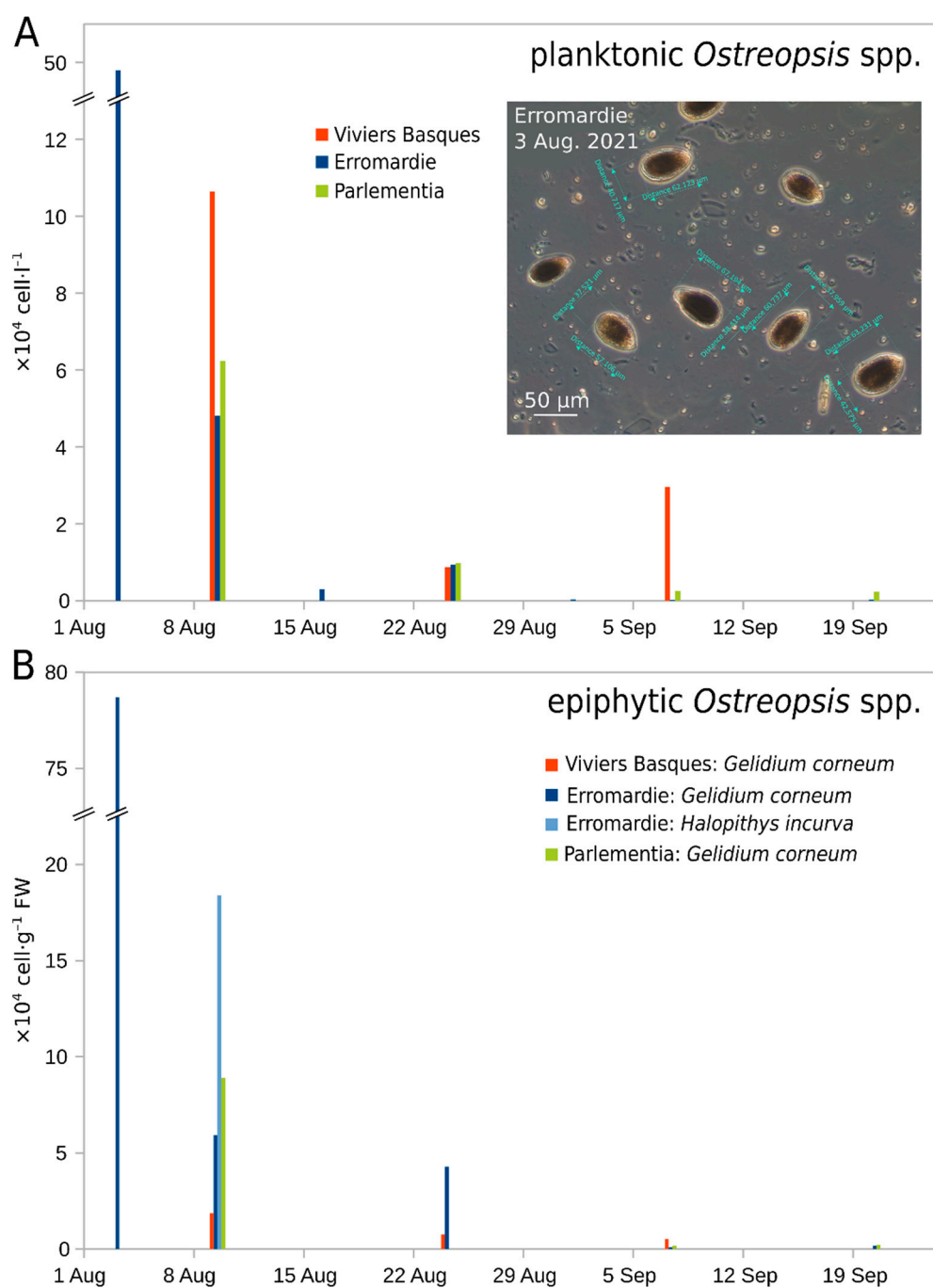


Figure 2. Abundances of *Ostreopsis* cells ((A), upper panel) and macroalgae ((B), lower panel) during summer 2021. The insert in (A) shows a micrograph of the Erromardie bloom water sample (3 August 2021) with many *Ostreopsis* cells fixed in Lugol's solution.

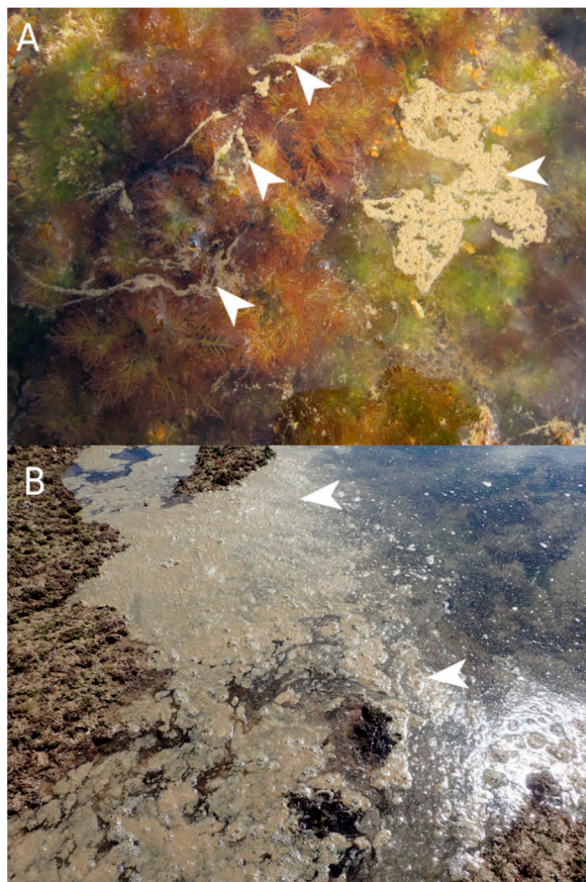


Figure 3. Scum-like aggregates (arrowheads) containing high concentration of *Ostreopsis* cells occasionally visible on the water surface in areas covered by macroalgae ((A), Alcyons beach, Guétary, 13 September 2021) or rocks ((B), Marbella beach, Biarritz, 10 September 2021).

2.2. Environmental Conditions before and during the 2020 and 2021 Events

As the intoxication phenomenon of beach users occurred twice, in the summers 2020 and 2021, albeit to a lower extent in 2020, it seemed worthwhile presenting here the environmental conditions for both years. Results of the meteorological and oceanographic parameters are shown using a timescale corresponding to the date of occurrence of the health disorders, where the date “0” corresponds to the day on which the reports of sickness began (4 September 2020 and 3 August 2021). Hence, this representation makes it possible to compare the environmental conditions during the weeks preceding the onset of the intoxication episodes of both years.

As shown in Figure 4, for both years, the prevailing winds during the weeks preceding the disease reports were onshore. While they were quite strong in the days preceding the 2020 event (end of August), the winds were weak before the 2021 bloom (July). In 2020, the wave height in the 15 days preceding the event was higher than in 2021. In both years, a drop in salinity levels of the surface water was observed from 8 to 15 days before the event. It was more marked in 2021 than in 2020, but bottom water salinities were stable and quite different in both years.

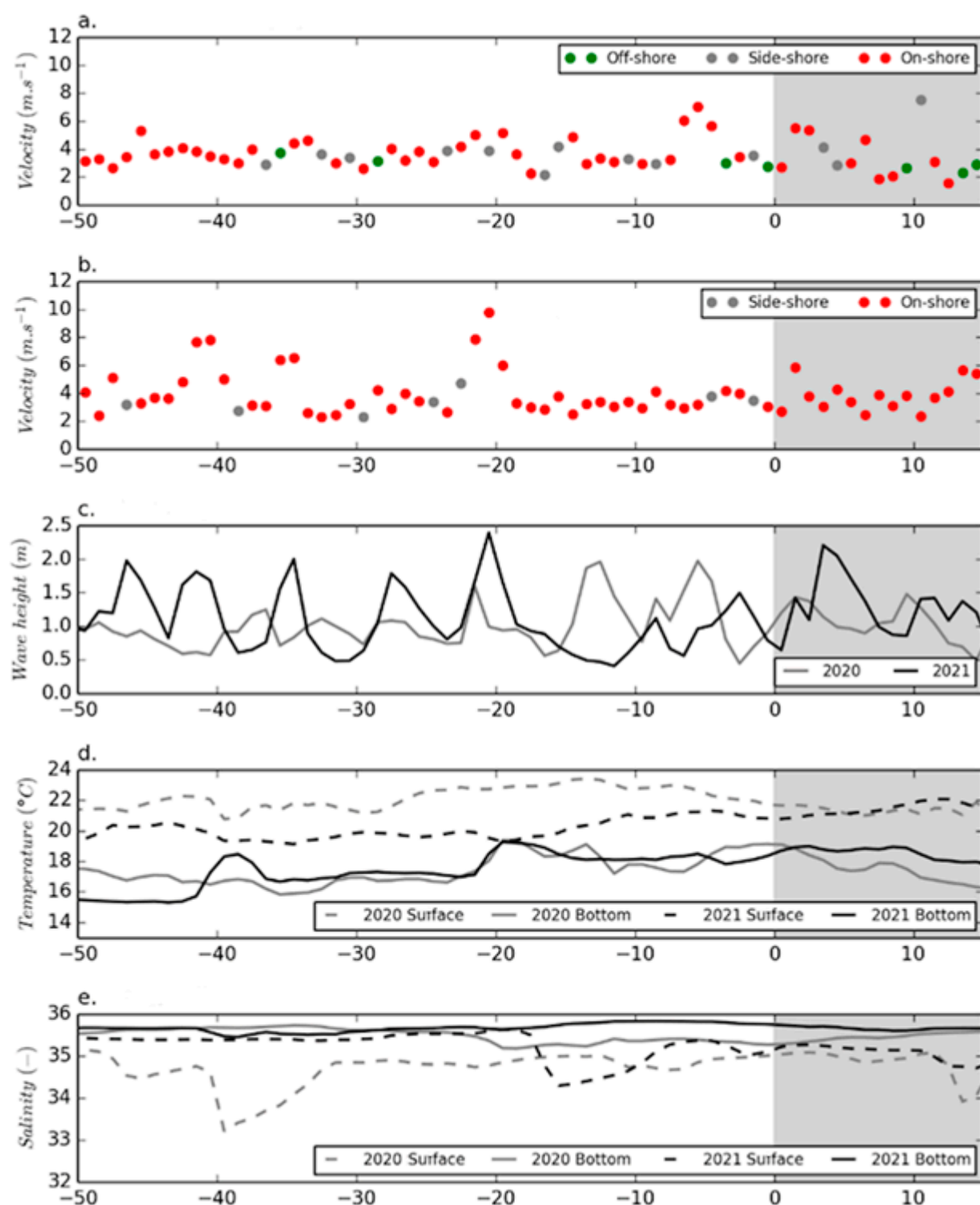


Figure 4. Temporal evolution of meteorological (wind velocity (a) in 2020; (b) in 2021) and oceanographic (wave height (c); water temperature (d); and salinity (e)) parameters (daily averages) before and at the beginning of both intoxication episodes (shown with gray background). For wind: onshore, coming from 240° to 360° ; offshore, coming from 60° to 180° ; side-shore, coming from 0° to 60° and 180° to 240° . The x-axis shows the number days before and after beginning of the toxic event (with 0 indicating the first intoxication report).

The only common feature of both years in terms of environmental conditions was the sudden rise in the bottom water temperature (above 18 °C) about 20 days before the appearance of symptoms in beach users. Thereafter, this temperature remained fairly high until the beginning of the event in 2020 and for 10 days after the event in 2021 (Figure 4).

2.3. Identification of *Ostreopsis* Species in the Bloom Samples

2.3.1. Cell Morphology in the 2020 Bloom Samples

During the 2020 bloom event, cells were only observed by light microscopy and by fluorescence to analyze their morphological features and plate pattern. Cells were typically tear-shaped, pointing ventrally, and their size was 55–72 µm deep and 35–50 µm wide, with a continuum of sizes. When observed in epifluorescence microscopy, the thecal plate pattern was typical of the genus, and no difference was seen among cells (Figure 5).

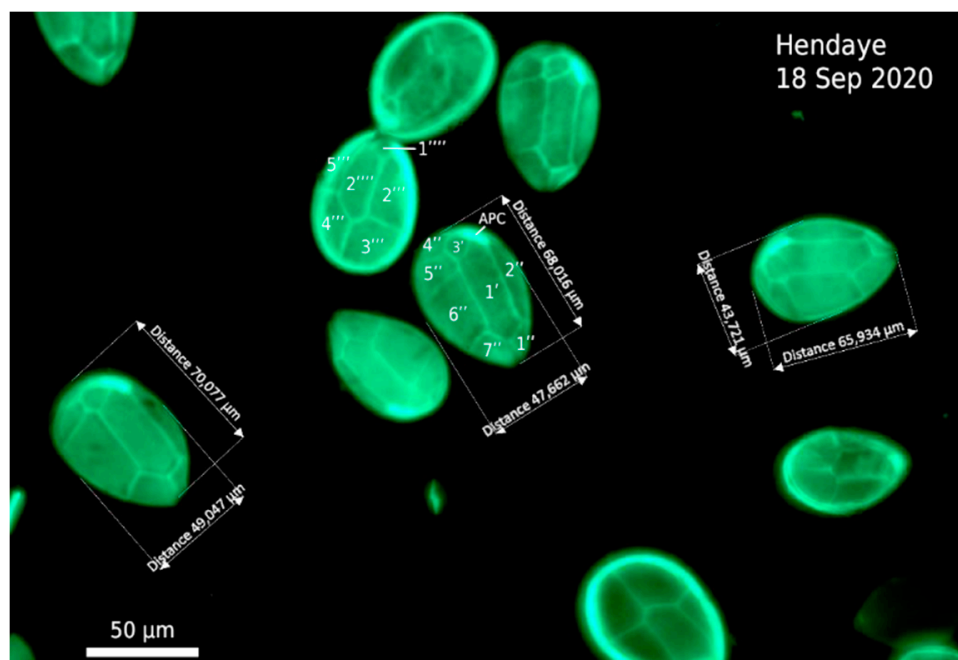


Figure 5. Epiphytic *Ostreopsis* cells from the Hendaye sample (18 September 2020) showing the shape, size, and thecal plate pattern after staining (Solophenyl Flavine 7GFE 500) and observation in epifluorescence microscopy. Scale bar = 50 µm.

2.3.2. Single Cells Isolated from the 2021 Environmental Sample and Estimation of Relative Abundances of *Ostreopsis* spp.

In order to identify species present in the environmental sample and estimate their relative abundance, 90 *Ostreopsis* cells were isolated randomly. When observed in light microscopy (LM), cells were teardrop-shaped, pointing ventrally ranging from 41.7 to 94.1 µm in depth (dorso-ventral length) and from 27.4 to 65.0 µm in width, with a continuum of sizes (Figures 6 and 7). Except these variations in size, all cells possessed a similar thecal pattern, and no distinctive feature could be observed in LM (Figure 6) or epifluorescence (not shown).



Figure 6. The 48 single *Ostreopsis* cells (on 90) isolated from the Errromardie bloom sample (16 August 2021) for molecular identification. Numbers indicate isolate number, while color corresponds to the obtained genotype: blue = *O. cf. ovata*; green = *Ostreopsis* sp. 9. Scale bar = 20 μm .

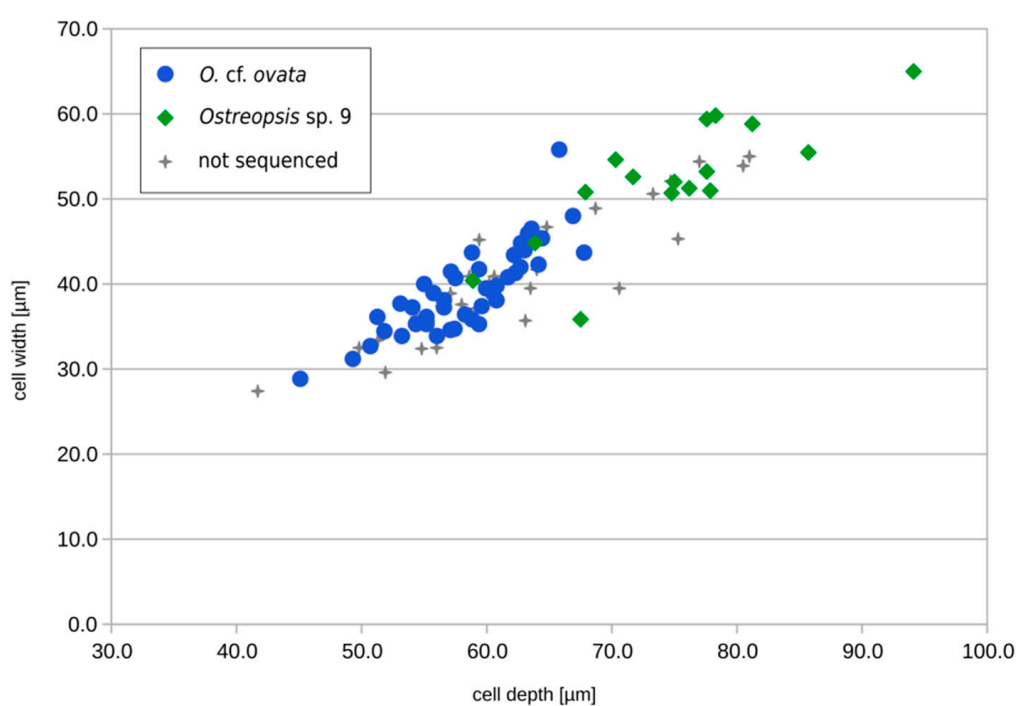


Figure 7. Size distribution of the 90 single cells isolated from the Errromardie environmental sample (16 August 2021) for morpho-molecular identification. Blue dots indicate specimens identified as *O. cf. ovata*, and green diamonds indicate specimens identified as *Ostreopsis* sp. 9 by sequencing of the ITS region. Specimens isolated but for which no sequence could be obtained ($n = 30$) are shown as gray crosses.

2.3.3. Molecular Phylogeny of Isolated Specimens and Cultivated Strains from the 2021 Bloom

Sequences obtained from both single cells isolated from an environmental sample ($n = 60$) and cultivated strains ($n = 3$) were used in a phylogenetic analysis for species/clade identification. In the maximum-likelihood (ML) tree obtained from the ITS region, 44 environmental sequences and one strain (IFR-OST-01E) grouped with ribotype 1 within subclade A of *O. cf. ovata*, while 16 environmental sequences and two strains (IFR-OST-02E, IFR-OST-03E) grouped with ribotype 22 within *Ostreopsis* sp. 9 (*O. cf. siamensis*) clade, indicating the co-occurrence of both species in the bloom (Figure 7).

As shown by the analysis (Table S1, Figure 8), the subclade A of *O. cf. ovata* includes sequences from various origins such as the Mediterranean Sea, Japan, Brazil (southwestern Atlantic), Canary Islands, and southern Portugal (Algarve, eastern Atlantic). Other subclades of *O. cf. ovata* included sequences from Australia, Asia (Viet Nam, Thailand, and Malaysia), Ecuador, and Belize. By contrast, all sequences of *Ostreopsis* sp. 9 showed a low level of divergence (Figure 8) although they originated from widely distant areas such as Australia, the Mediterranean Sea, Portugal, and the Basque coast (Atlantic coast of Spain and France).

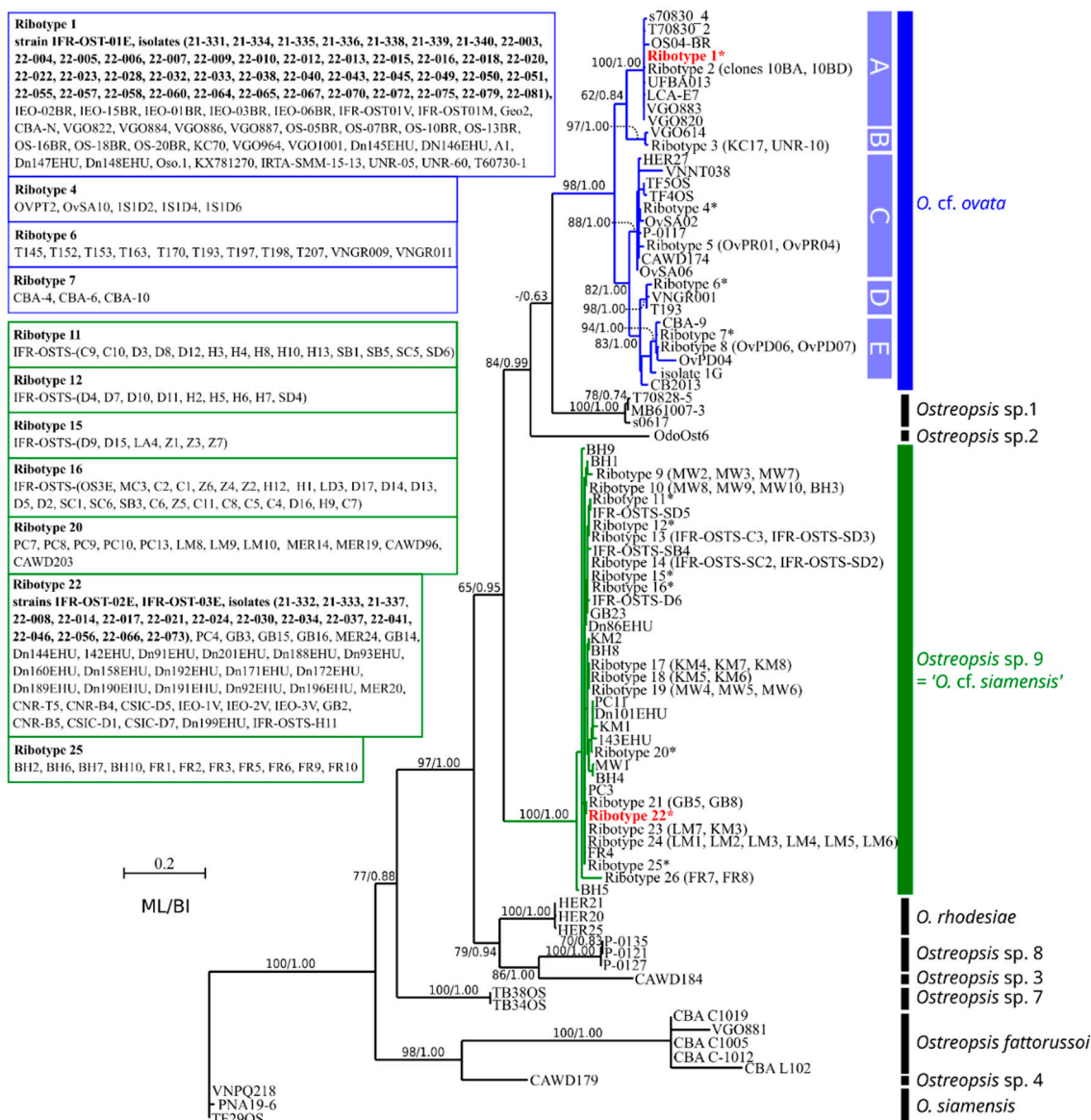


Figure 8. Maximum-likelihood phylogenetic tree inferred from ITS region sequences of various *Ostreopsis* strains and field specimens (88 sequences, 693 sites). Identical sequences are considered to belong to a single ribotype (the list of all sequences used in the analysis is given in Supplementary Table S1). * indicates ribotypes for which sequences are listed in boxes on the left. A–E correspond to subclades in *Ostreopsis* cf. *ovata* clade. Sequences acquired in this study are in bold face. Numbers at nodes indicate bootstrap values (in ML analysis) and posterior probabilities (Bayesian inference). Bootstrap values below 65 are indicated by '-'.

2.4. Toxin Profiles of *Ostreopsis* Samples

Toxin profiles were determined from environmental samples during the 2021 bloom of *Ostreopsis* spp., as well as from extracts of the three cultivated strains of *Ostreopsis* spp. isolated during the same bloom. Twenty known metabolites produced by *Ostreopsis* spp. were targeted (Table S2) by LC–MS/MS analysis: (i) palytoxin group (PLTX, isob-PLTX, 42-OH-PLTX); (ii) ovatoxin group (OVTX-a to -k); (iii) ostreocins (OST-a, -b, -d, -e); (iv) mazarenotoxin group (McTX-a, -b, -c). Only the PLTX standard is commercially available; the other molecules were, therefore, sought in MRM (mode multiple reaction monitoring) acquisition (i.e., targeted quantitative analysis) on the basis of transitions of published or deduced molecular masses (Table S2).

2.4.1. Toxins Detected in the 2021 Environmental Sample from Erromardie (16 August 2021)

Among all metabolites targeted in the study, only two molecules, OVTX-a and -b were quantified in the analyzed environmental sample (Figure 9, Table 1). The intracellular concentration was calculated on the basis of the total abundance of *Ostreopsis* cells in the water (Figure 9, Table 1).

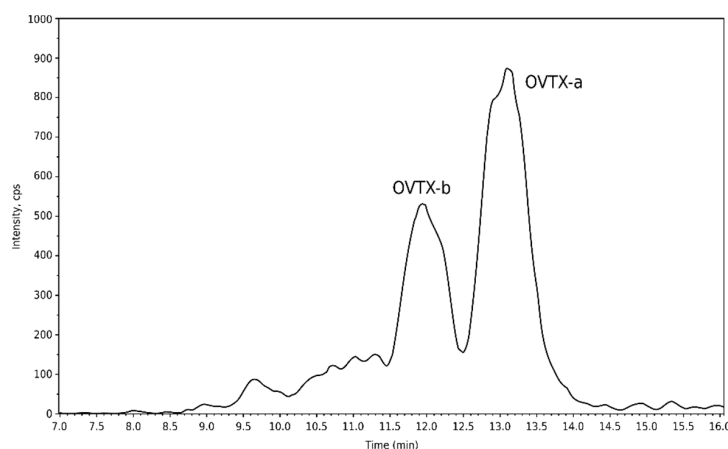


Figure 9. Chromatogram of LC–MS/MS analysis of the sampled bloom from Erromardie (16 August 2021).

Table 1. Toxins quantified in the environmental bloom sample from Erromardie (16 August 2021). The concentrations are indicated in PLTX equivalents.

Sample Analyzed	Toxins	Cellular Content (fg eq. PLTX·Cell ⁻¹)
Bloom water sample (16 August 2021)	OVTX-a OVTX-b	5.5 ¹ 2.3 ¹

¹ Based on the total abundance of *Ostreopsis* cells in the sample.

2.4.2. Toxin Profiles of Cultivated Strains

Culture extracts from the three *Ostreopsis* strains were analyzed, and, among the targeted toxins, only the ovatoxins (OVTX-a, -b, -c, -d, -e) were quantified in strain IFR-OST-01E identified as *Ostreopsis cf. ovata* (Figure 10, Table 2). The concentrations obtained are indicated in PLTX equivalents. No targeted toxin was detected in extracts of the two other strains (IFR-OST-02E and IFR-OST-03) identified as *Ostreopsis* sp. 9 (*O. cf. siamensis*) (Table 2).

Table 2. Toxins quantified in cultured strains of *Ostreopsis* from Erromardie bloom. The concentrations are indicated in PLTX equivalents.

Strain	Species	Concentrations (pg eq. PLTX·Cell ⁻¹)					Cell Concentration (Cells·mL ⁻¹)
IFR-OST-01E	<i>Ostreopsis cf. ovata</i>	OVTX-a 4.3	OVTX-b 1.6	OVTX-c 0.2	OVTX-d 0.3	OVTX-e 0.3	80,700
IFR-OST-02E	<i>Ostreopsis</i> sp. 9 (<i>O. cf. siamensis</i>)	No targeted toxins detected					96,300
IFR-OST-03E	<i>Ostreopsis</i> sp. 9 (<i>O. cf. siamensis</i>)	No targeted toxins detected					84,000

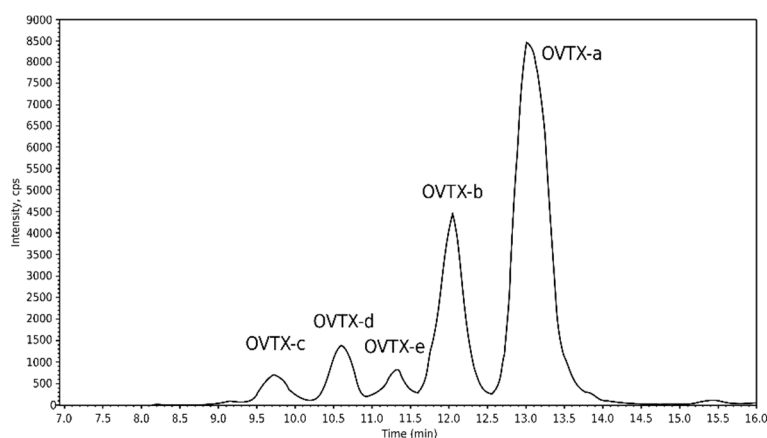


Figure 10. Chromatogram from LC–MS/MS analysis of the strain IFR-OST-01E (*O. cf. ovata*) isolated from Erromardie sample.

3. Discussion

3.1. *Ostreopsis* Bloom Events and Impact on Human Health

As shown by our data, massive respiratory symptoms reported in early August 2021 were concomitant with maximal abundances of *Ostreopsis* spp. observed in the water column and on macroalgae, allowing the health disorders to be associated with the bloom event. The high number of 674 analyzed cases of illness indicates a very important phenomenon on beaches of the Basque coast, and it cannot be excluded that it affected even more people who did not report their symptoms to medical services. In light of this exceptional event, the scarce reports from 2020 could putatively be linked to an *Ostreopsis* outbreak in September; however, due to its late occurrence and the low number of reports, it was not further investigated nor drove specific sampling for molecular and toxins analyses. Hence, a direct link remains hypothetical.

The symptoms reported from the French Basque coast in 2021 (and, to a lesser extent, in 2020) are in perfect agreement with the clinical picture reported in Mediterranean areas [5]. According to the literature, it is probable that PLTX-like toxins (OVTXs) could be at the origin of the observed symptoms of respiratory disorders [51]. Indeed, this type of symptom was already observed in people exposed to aerosols from aquariums containing *Palythoa*, where it is used as a decorative element [53,72]. The reported cases of exposure to PLTX in this context are increasing in Europe and the United States [52,73]. The presence of PLTX-like OVTX-a and isob-PLTX (putative) has been shown in aerosols during an *Ostreopsis* bloom but at a very low concentration (2.4 pg of ovatoxins per liter of air) [27]. Other authors have suggested that fragments of *Ostreopsis*, mucus and/or associated microorganisms (e.g., bacteria) could be present in the aerosol and cause respiratory disorders [56,74].

To date, only blooms of *O. cf. ovata* producing OVTXs have been associated with such symptoms occurring in humans, and other species have not caused such health issues although they can form blooms and reach high abundances. For instance, it is now established that the tropical toxic species *O. siamensis* can form benthic blooms and produce ostreocins [18], but effects of these molecules are yet unknown, and their toxicity has only been demonstrated by mouse and neuro-2a cell bioassays [18,43].

3.2. Environmental Conditions Associated with the 2020 and 2021 Bloom Events

In 2021, reports of symptoms occurred about 1 month earlier (early August) than in 2020 (in September). Moreover, the detection of the 2021 bloom was primarily initiated by first reports of health issues, and it probably started even earlier in July. Unfortunately, no abundance data of *Ostreopsis* spp. are available for the initiation phase of the bloom, and the complete dynamics remains unknown. Only a decrease in abundances in water (planktonic cells) and on macroalgae (epiphytic cells) was observed from the beginning of August onward. Analysis of environmental parameters before and during the bloom events of both

2020 and 2021 did not allow identifying a specific pattern common for both years, except a rather high seawater temperature (surface exceeding 20 °C and bottom exceeding 18 °C) for a long period before the bloom. Because *Ostreopsis* cells grow on macroalgae attached to rocky bottoms in shallow waters, temperature is generally identified as determining seasonal trends and abundances of this genus [75,76]. In the north of Spain and Basque country, at least three consecutive months with a sea surface temperature exceeding 19.5 °C were identified as a putative trigger of *Ostreopsis* development [77]. Hence, this parameter could be significant, but it needs verification by longer time series in subsequent years.

3.3. Identification of *Ostreopsis* Species during the 2021 Toxic Event

Observed by light microscopy, samples from the blooms of 2020 and 2021 were found to contain abundant *Ostreopsis* cells, but a continuum in body sizes and similar thecal plate pattern did not allow conspicuously identifying different morphotypes. Consequently, species present in the 2020 sample remained unidentified. Due to poor morphological features to distinguish species and the overlap of size ranges, a reliable identification at species level is only possible using molecular methods [14–16,21], which was possible only with the 2021 sample. As shown by our results combining morphometric and genetic data, while larger specimens can be attributed to *Ostreopsis* sp. 9 (*O. cf. siamensis*) and smaller ones to *O. cf. ovata*, the majority of cells in the medium range (depth ca. 60–70 µm) could not be identified solely by light microscopy and required a molecular analysis.

According to sequences acquired from single cells and isolated strains, our study demonstrated the presence of two *Ostreopsis* species in the Erromardie bloom on the French Basque coast. As shown by the phylogenetic analysis, sequences of *Ostreopsis* sp. 9 from the bloom belonged to ribotype 22, which includes other strains previously isolated from Saint-Jean-de-Luz (another site on this French Basque coast), such as Dn201EHU, Dn171EHU, Dn172EHU, and several others originating from the Spanish Basque coast [67] (Table S1), not far from Erromardie beach. Hence, the presence of cells of this ribotype in the 2021 bloom sample is not surprising, since it has been reported in the area for several years [66,67,70]. In a more recent study, a real-time polymerase chain reaction (RT-PCR) approach on many sampling sites confirmed previous observations, and this species was found in several sites between Comillas (Spain) and Biarritz (France) [71]. Furthermore, although no cells could be observed to the north of Biarritz, results from RT-PCR showed that eDNA of *Ostreopsis* sp. 9 has a wider distribution area in the Bay of Biscay, since it could be detected in other sites in the median part of the Bay (Aquitaine) and up to Brittany [71]. Interestingly, no other *Ostreopsis* species have been detected in a previous study in north Spain and Basque coasts, and *Ostreopsis* sp. 9 (*O. cf. siamensis*) was considered to be the unique *Ostreopsis* species present in this part of Bay of Biscay [70] until the present work.

It is notable that, although the name *O. cf. siamensis* has been widely used for many years for this genotype, it has recently been shown that it differs widely from *O. siamensis*, the type species of the genus, found in tropical areas [18,19]. Since the two organisms are clearly separated, in order to avoid further confusions [2], it has been suggested to use a different name for this genotype; in the present study, we implement the use of a numbered genotype label introduced recently [19].

Interestingly, our genetic analysis demonstrates unambiguously that cells of another genotype, *O. cf. ovata* (subclade A), were co-occurring in the 2021 bloom sample. This is, to our knowledge, the first evidence of the presence of this species on the Basque coast and in the Bay of Biscay. In a recent study based on eDNA and RT-PCR methods, where numerous samples collected in summer 2018 on the Spanish and French Basque coast were analyzed, no positive result was obtained for *O. cf. ovata* [71]. Given the sensitivity of the method, this indicates that, if present, this species was below the detection limit, and it is probably rare. In light of these data, the hypothesis of a recent introduction and installation of *O. cf. ovata* in this part of the Bay of Biscay cannot then be rejected, since, before 2020, *Ostreopsis* proliferations were not associated with human poisonings (Regional Health Agency, pers. com.).

The present data allow extending the distribution area of *O. cf. ovata* to the Atlantic Ocean, since, prior to this study, *O. cf. ovata* was not reported north of Algarve, in the south of Portugal [67–69], for the eastern Atlantic. Hence, the present study allows extending the northern distribution limit of this species in the northeastern Atlantic from the southwestern coast of the Iberian Peninsula (Algarve) to the Cantabrian Sea in the Bay of Biscay (French Basque coast).

The co-occurrence of two species in the Erromardie bloom sample is in agreement with previous findings; *O. cf. ovata* (subclade A) was found to co-occur with *Ostreopsis* sp. 9 (e.g., in the Mediterranean Sea, Brazil [14,59], as well as in the Azores and south Portugal [62,67]). From an ecological point of view, the latitude of Erromardie beach (Basque coast) (43.4° N) is comparable with some of the Mediterranean areas where *O. cf. ovata* was found to form massive blooms, such as Genoa on the Ligurian coast or the Adriatic coast [14,29]. However, the conditions in the Atlantic Ocean are drastically different from those in the Mediterranean Sea, mostly because of a strong tidal effect and different macroalgal communities in both areas. However, there are several reports of blooming *O. cf. ovata* in warm regions of the Brazilian Atlantic coast, where the tidal effect is also present, which suggests that temperature might be a more important factor explaining the distribution of this species [60,61].

Further ecological studies aiming at understanding the population dynamics and ecological preferences of both *Ostreopsis* species in the Basque coast should address this question in the future, as it is important for bloom and risk anticipation. Indeed, experimental work in the field and in the laboratory must be carried out to study the dynamics of bloom development and the factors that influence the growth, toxin production, and spatiotemporal distribution of both species on the Basque coast (e.g., temperature, hydrodynamics, nutrients, type of substrate, and salinity).

3.4. Toxin Production by *Ostreopsis* Species during the 2021 Toxic Event

The presence of OVTXs in both environmental and cultivated samples corroborated the identification of *O. cf. ovata* as the producer, since these molecules have not been detected for *Ostreopsis* sp. 9. Our analysis on isolated strains confirmed that OVTX was only present in strain IFR-OST01E of *O. cf. ovata* and absent in the other strains of *Ostreopsis* sp. 9. The monoclonal culture IFR-OST-01E of *O. cf. ovata* contained higher concentrations (on the order of $\text{pg}\cdot\text{cell}^{-1}$ vs. $\text{fg}\cdot\text{cell}^{-1}$ for the environmental sample), as well as a more complete toxin profile (OVTX-a to -e vs. OVTX-a and -b for the environmental sample). This particular toxin profile, with a dominance of OVTX-a followed by OVTX-b and a minor presence of OVTX-c and -d, has already been identified in strains of *O. cf. ovata* from the Mediterranean Sea and Brazil [39,60,61,78], all genetically belonging to subclade A. The analysis of the toxin profile of 55 strains of *O. cf. ovata* collected in the Mediterranean Sea indicates qualitative variability and intraspecific quantitative toxin content [37]. Except for one unique strain, all strains produced OVTXs: 67% strains contained OVTX-a through -e, OVTX-g, and isobaric PLTX; 25% contained OVTX-a, -d, and -e, and isobaric PLTX; 4% produced only OVTX-b and -c; a single compound profile contained OVTX-a to f, with a dominance of OVTX-f, and isobaric PLTX. The OVTX-l analogue was detected in 36 strains [37]. Compared with reports from other areas, the estimated toxin content observed in strain IFR-OST01E ($6.7 \text{ pg}\cdot\text{cell}^{-1}$) is within the same order of magnitude as strains from the Mediterranean Sea reported with OVTXs mostly between 4 and $70 \text{ pg}\cdot\text{cell}^{-1}$, up to $238 \text{ pg}\cdot\text{cell}^{-1}$ [37]. However, the estimated concentration is low in comparison to some Brazilian *O. cf. ovata* strains containing $31\text{--}468 \text{ pg}\cdot\text{cell}^{-1}$ [61,79] and high in comparison to some strains from the Pacific [41,42]. Comparatively, the apparently low intracellular toxin content observed in the environmental sample ($7.8 \text{ fg}\cdot\text{cell}^{-1}$) can be explained by the presence of both toxic *O. cf. ovata* and nontoxic *Ostreopsis* sp. 9, impossible to distinguish in cell counts by LM. According to sequences obtained from single-cells randomly isolated in the bloom sample, *O. cf. ovata* appeared to be relatively more abundant (72%) than *Ostreopsis* sp. 9 (28%) in the sample collected 16 August 2021. Since no samples allowing

further molecular analysis and toxin analysis were collected earlier, the temporal dynamics of both species and the toxin content during the bloom could not be analyzed. This would be important in future studies since it has been shown that toxin content is dependent on the bloom phase [78].

As previously reported, for instance, for the Mediterranean (Italy) and Atlantic (Portugal) strains of *Ostreopsis* sp. 9 [80], none of the targeted toxins analyzed in this study could be identified in both strains of *Ostreopsis* 9 isolated from the Basque coast. Indeed, it has been suggested that this species presents a much lower risk to human health than *O. cf. ovata*, which produces comparatively high levels of PLTX-like compounds [80]. On the basis of cellular assays, a study reported that crude extracts of *Ostreopsis* sp. 9 from several locations along the Andalusian coast contained highly active PLTX-like toxins and may be considered as a possible risk to humans [81], but no compound could be identified. Bioassays on *Artemia franciscana* crustaceans revealed allelopathic effects caused by *Ostreopsis* sp. 9 isolated on the Basque coast, despite the absence of detection of known toxins [82]. In addition, some strains of *Ostreopsis* sp. 9 from southeast Australia were found to produce other than PLTX-like analogues at a very low level (about $0.17 \text{ pg} \cdot \text{cell}^{-1}$), and they had toxic effects on mice intraperitoneally with a very high dose of extract (LD_{50} of $25 \text{ mg} \cdot \text{kg}^{-1}$) of the studied strain, versus only 0.15 to $0.72 \text{ } \mu\text{g} \cdot \text{kg}^{-1}$ for PLTX [83]. Hence, it is highly probable that nonidentified toxic compounds in this species cause negative effects on marine benthic organisms, but this is considerably less studied than for *O. cf. ovata* [84] and further work is necessary.

4. Materials and Methods

4.1. Sampling on the Basque Coast

In 2020, one macroalgal sample (*Ericaria selaginoides*) was collected at Hendaye on 18 September (Figure 1, Table S3). In 2021, after first reports of symptoms (2 August 2021), water and macroalgae were collected at Erromardie beach (Figure 1), and, since the phenomenon was extending to other areas, other samples were collected at two other beaches (Viviers Basque, Parlementia) during the following weeks (Figure 1). Table S3 summarizes the samples collected for the different analyses realized in the study.

Water samples were collected using 500 mL plastic flasks sunk into the water at a depth of about 30 cm in the vicinity of attached macroalgae. Macroalgal samples were collected with surrounding water at a depth of about 30 cm, using 250 mL plastic flasks. After shaking the bottle for about 5 min, the macroalgae were removed and drained, and their fresh weight (FW) was measured. Epiphytic cells collected were fixed with acidic Lugol's solution (2% v/v) for abundance estimations of *Ostreopsis* cells.

Water samples for cell counts were fixed with acidic Lugol's solution (2% v/v) and stored in the dark. For molecular identification of *Ostreopsis* cells, the sample was fixed with 95% ethanol (final concentration) and stored at 4 °C. For isolating strains, samples were kept fresh with no direct exposure to light.

For toxin analysis of water samples, after counting the cells, 60 L of seawater was filtered through a 47 mm GF/F filter (Whatman) (Erromardie, 16 August 2021, Table S3) in duplicate, and the two filters were kept frozen at –20 °C until analysis.

4.2. Cell Counts and Estimation of *Ostreopsis* Abundances

Cells from the Lugol-fixed samples were observed using a Zeiss Axio Observer microscope (Carl Zeiss, Oberkochen, Germany) equipped with a digital camera. Counts were realized in 10 mL settling chambers at ×100 magnification and using phase-contrast optics. For visualization of the thecal plates, cells were stained with Solophenyl Flavine 7GFE 500 and observed in epifluorescence microscopy with the same microscope equipped with a GFP filterset [85].

4.3. Environmental Parameters

Environmental parameters were obtained from different meteorological and oceanographic models; wind speed and direction were results from the AROME regional model (Meteo France forecasting system, spatial resolution of 2500 m), wave height was from WaveWatchIII simulations for the NORGAS_UG configuration (spatial resolution of 500 m), and water temperature and salinity were from MARS3D simulations for the MANGAE_2500 configuration (spatial resolution of 2500 m) [86].

4.4. Strains Isolation and Cultivation

Cells were isolated with a micropipette using an inverted IM35 microscope (Carl Zeiss, Oberkochen, Germany), rinsed in several drops of filtered seawater, and put in the well of a four-well microplate (Thermo Scientific®, Waltham, MA, United States). Three monoclonal strains of *Ostreopsis* spp. were grown in L1 culture medium [87] prepared with filtered seawater at pH 8.2 and a salinity of 35. They were maintained in 250 mL Erlenmeyer flasks placed in a thermoregulated room at 17 °C and under 160 $\mu\text{mol}\cdot\text{quanta m}^{-2}\cdot\text{s}^{-1}$ PAR (photosynthetically active radiation) on a 16 h light/8 h dark cycle. Irradiance was delivered by Osram Fluora 36W (Munich, Germany) and Philips Daylight 36W (Amsterdam, the Netherlands) lamps.

4.5. Species Identification and Estimation of Their Relative Abundances

To identify species present during the bloom, sequencing of the ITS1-5.8S rDNA-ITS2 (ITS region) was realized on single cells isolated both from the ethanol-fixed environmental sample and from strains in culture.

4.5.1. Single-Cells Isolation

For identification and a rough estimation of the relative abundance of *Ostreopsis* spp. In the ethanol-fixed bloom sample (16 August 2021), 90 single cells were isolated randomly from a 5 mL subsample settled in a sedimentation chamber using an IX51 (Olympus, Tokyo, Japan) inverted microscope. Cells were isolated with a glass micropipette, transferred to a microscope slide, photographed to record their overall morphology, rinsed in several drops of ultrapure deionized water, and then transferred into a 0.2 mL PCR tube for molecular analysis.

4.5.2. DNA Extraction from Strains

The three live cultures (IFR-OST-01E, IFR-OST-02E, and IFR-OST-03E) were extracted with the PCR BIO Rapid Extract PCR Kit (PCR Biosystems Ltd., London, United Kingdom) which combines extraction and PCR. A volume of 70 μL of culture was transferred into a 0.5 mL tube and centrifuged for 3 min at 14,000 $\times g$. The supernatant was discarded to retain only the pellet. Then, the manufacturer's instructions were followed except for the dilution step where 190 μL of water was added instead of the recommended 900 μL . The pair of primers used for the PCR was ITS-FW (GTAGGTGAAACCTGCGGAAGG) and D3B (TCGGAGGGAACCAAGCTACTA) [88,89].

4.5.3. Amplification and Sequencing

For PCR, the tubes were processed as described previously [18] using Promega Master Mix (Promega, France) according to the manufacturer's instructions. Thermal cycling conditions comprised an initial 2 min heating step at 95 °C, followed by 35 cycles of 95 °C for 30 s, 60 °C for 60 s, 72 °C for 120 s, and a final extension at 72 °C for 5 min. Positive samples revealed by visualization on an agarose gel (2%) after electrophoresis were selected for sequencing. A purification using the ExoSAP-IT Product Cleanup reagent (Affymetrix, Cleveland, OH, USA) was realized prior to the sequencing reaction with Big Dye X-terminator v. 3.1 Sequencing Kit (Applied Biosystems, Foster City, CA, USA). Excess labeled nucleotides were removed using a Bid Dye X-terminator purification kit,

and sequencing products were run on an ABI PRISM 3130 Genetic Analyzer. Forward and reverse reads were obtained.

4.5.4. Phylogenetic Analysis

Prior to phylogenetic analysis inferred from the ITS1-5.8S rDNA-ITS2 region, *Ostreopsis* sequences related to those obtained in the study were identified using the BLAST tool of NCBI. In addition to the 48 sequences acquired, a total of 267 sequences were retrieved from GenBank (Table S1) including 82 sequences for *O. cf. ovata* and 163 sequences for *Ostreopsis* sp. 9 (*O. cf. siamensis*; Table S1). In order to limit the number of repeated sequences in the analysis, when multiple clones share a similar sequence, they were considered as a single ribotype. Hence, the dataset used for phylogenetic analysis included 88 sequences. Sequences were aligned using MAFFT v. 7 with the q-ins-i option [90] and manual refinement. Maximum-likelihood analysis was performed using PHY-ML v. 3.0 software [91], and a bootstrap analysis (1000 pseudoreplicates) was used to assess the relative robustness of branches of the ML tree. In addition, a Bayesian inference (BI) analysis was run using MrBayes v. 3.1.2 [92].

4.6. Toxin Analysis by Liquid Chromatography Tandem Mass Spectrometry (LC–MS/MS)

Samples were screened for the presence of PLTX and related analogues (20 analogues; see Table S2).

4.6.1. Sample Preparation

- Environmental sample

In order to extract environmental *Ostreopsis* cells collected on the filters, the two GF/F filters were thawed. Then, 3 mL MeOH was added to each filter, and the filters were ultrasonicated in an ultrasonic bath at 25 Hz for 5 min. Then, after centrifugation (4300×*g* for 5 min at 6 °C), the resulting pellet was extracted again with 2 mL of MeOH, both supernatants were pooled, and the volume was adjusted to 5 mL, before analysis by LC–MS/MS.

- Strains in culture

Pellets of the three *Ostreopsis* strains (containing approximately 85,000 cells·mL⁻¹), were extracted with 500 µL of MeOH using an ultrasonic bath at 25 Hz for 10 min. After centrifugation (4300×*g* for 5 min at 6 °C), the resulting pellet was extracted twice with 500 µL MeOH, both supernatants were pooled, and the volume was adjusted to 1 mL. The supernatants were then analyzed by LC–MS/MS.

4.6.2. LC–MS/MS Analysis

The supernatants were ultrafiltered (0.20 µm, Nanosep MF, Pall, Mexico) before LC–MS/MS analyses. Liquid chromatography was performed on a Poroshell 120 EC-C18 column (100 × 2.1 mm, 2.7 µm, Agilent, Les Ulis, France) equipped with a guard column (5 × 2.1 mm, 2.7 µm, same stationary phase) using a Nexera Ultra-Fast Liquid Chromatography system (Prominence UFLC-XR, Shimadzu, France). Gradients of water (A) and acetonitrile 95% (B) both containing 0.2% acetic acid were used at a flow rate of 0.2 mL·min⁻¹. The injection volume was 5 µL, and the column temperature was 25 °C. MS/MS analyses were performed with an API 4000QTRAP (AB Sciex, Les Ulis, France) in positive ion mode and using MRM (Multiple Reaction Monitoring) acquisition. UV detection at 220, 233, 263, and 220–360 nm was performed with a diode array detector (Prominence, SPD-M20A, Shimadzu, France).

Lastly, methods described in [16] were used to detect PLTX, 42-OH-PLTX, 12 OVTXs (-a to -k), four OSTs (-A, -B, -D, and -E1), and three McTXs (A to C), corresponding to 20 compounds [16]. The used precursors and product ions used, as well as wavelengths for detection of these compounds, were similar to those used in [16]. Quantification was performed relative to the PLTX standard (Wako Chemicals GmbH, Germany) using a nine-

point calibration curve. The limits of detection and quantification were 20 and 30 ng·mL⁻¹ for the PLTX standard.

5. Conclusions

As revealed by our analysis, the toxic *Ostreopsis* bloom, which occurred in summer 2021 on the French Basque coast and affected about 700 people, was not monospecific and included two species: *Ostreopsis* sp. 9 (*O. cf. siamensis*) and *O. cf. ovata*. From this result, it can be suspected that a similar bloom caused the health disorders reported in September 2020, but the low number of cases did not match the massive issues in 2021. While the former is a well-known species reported in the area for several years but usually with no noticeable effects on the population, the latter was found for the first time in this part of Bay of Biscay. Interestingly, *O. cf. ovata* was not previously detected in this area despite a sampling in 2018 at a large geographical scale on the French Atlantic coast and the use of sensitive molecular methods in a previous study in 2018 [71]. Hence, the hypothesis of a recent introduction cannot be excluded, and the presence of this invasive dinoflagellate might cause new problems in the future, in relation to global warming. This problematic species, well established in the Mediterranean Sea, as well as on the southwestern Atlantic (Brazilian coasts) extends its distribution area in the northern Atlantic. The toxin profile with OVTX-a and -b as predominant compounds in the environmental sample corroborates the presence of *O. cf. ovata*, since these molecules have only been found in this species, and they were likely produced by this taxon in the bloom, as revealed by analysis of clonal strains. Furthermore, it would be important to analyze the cytotoxic effects of both species on human and marine fauna using bioassays. Such approaches are required to better evaluate the toxic risk associated with *Ostreopsis* blooms on the Basque coast.

Supplementary Materials: The following supporting information can be downloaded at <https://www.mdpi.com/article/10.3390/md20070461/s1>: Table S1, List of strains and sequences used in the phylogenetic analysis; Table S2, Molecular ion transitions (Q1 > Q3) and wavelengths used for the detection of palytoxin and its analogues (ovatoxins, ostreocins, and mazarenotoxins) [31,33–36,44,46,47,80,93–97]; Table S3, Summary of samples collected for the different analyses.

Author Contributions: Conceptualization, N.C. and Z.A.; methodology, N.C., V.S., F.H., M.-N.d.C. and Z.A.; formal analysis: F.G.; investigation, N.C., E.A., I.A., G.B., L.C., M.-N.d.C., F.H., M.L., C.M., C.P., M.P.-R., F.S., V.S. and Z.A.; writing—original draft preparation, N.C. and Z.A.; writing—review and editing, C.P., I.A., V.S., N.C. and Z.A.; visualization, M.-N.d.C., C.M. and F.S.; supervision, Z.A. and N.C.; project administration, Z.A. All authors have read and agreed to the published version of the manuscript.

Funding: This research received no external funding.

Institutional Review Board Statement: Not applicable.

Data Availability Statement: Not applicable.

Acknowledgments: The authors thank the technical staff of Ifremer laboratories (LER-AR, LER-BO, and PHYTOX) for helping with sample analyses, without whom these data would not exist. The authors also extend special thanks to K. N. Mertens for carefully rereading the manuscript and improving the language usage.

Conflicts of Interest: The authors declare no conflict of interest.

References

1. Schmidt, J. Flora of Koh Chang: Contribution to the Knowledge to the Vegetation in the Gulf of Siam. Part IV. Peridiniales. *Bot. Tidsskr.* **1901**, *24*, 212–221. [[CrossRef](#)]
2. Tester, P.A.; Litaker, R.W.; Berdalet, E. Climate Change and Harmful Benthic Microalgae. *Harmful Algae* **2020**, *91*, 101655. [[CrossRef](#)]
3. Neves, R.A.F.; Contins, M.; Nascimento, S.M. Effects of the Toxic Benthic Dinoflagellate *Ostreopsis* cf. *ovata* on Fertilization and Early Development of the Sea Urchin *Lytechinus variegatus*. *Mar. Environ. Res.* **2018**, *135*, 11–17. [[CrossRef](#)] [[PubMed](#)]

4. Pavaux, A.-S.; Rostan, J.; Guidi-Guilvard, L.; Marro, S.; Ternon, E.; Thomas, O.P.; Lemée, R.; Gasparini, S. Effects of the Toxic Dinoflagellate *Ostreopsis* cf. *ovata* on Survival, Feeding and Reproduction of a Phytal Harpacticoid Copepod. *J. Exp. Mar. Biol. Ecol.* **2019**, *516*, 103–113. [CrossRef]
5. Tichadou, L.; Glaizal, M.; Armengaud, A.; Grossel, H.; Lemée, R.; Kantin, R.; Lasalle, J.-L.; Drouet, G.; Rambaud, L.; Malfait, P.; et al. Health impact of unicellular algae of the *Ostreopsis* genus blooms in the mediterranean sea: Experience of the French Mediterranean coast surveillance network from 2006 to 2009. *Clin. Toxicol.* **2010**, *48*, 839–844. [CrossRef] [PubMed]
6. Tubaro, A.; Durando, P.; Del Favero, G.; Ansaldi, F.; Icardi, G.; Deeds, J.R.; Sosa, S. Case Definitions for Human Poisonings Postulated to Palytoxins Exposure. *Toxicon* **2011**, *57*, 478–495. [CrossRef] [PubMed]
7. Durando, P.; Ansaldi, F.; Oreste, P.; Moscatelli, P.; Marensi, L.; Grillo, C.; Gasparini, R.; Icardi, G.; Collaborative Group for the Ligurian Syndromic Algal Surveillance. *Ostreopsis ovata* and Human Health: Epidemiological and Clinical Features of Respiratory Syndrome Outbreaks from a Two-Year Syndromic Surveillance, 2005–2006, in North-West Italy. *Euro Surveill.* **2007**, *12*, 3212.
8. Vila, M.; Abós-Herràndiz, R.; Isern-Fontanet, J.; Àlvarez, J.; Berdalet, E. Establishing the Link between *Ostreopsis* cf. *ovata* Blooms and Human Health Impacts Using Ecology and Epidemiology. *Sci. Mar.* **2016**, *80*, 107–115. [CrossRef]
9. Aligizaki, K.; Katikou, P.; Nikolaidis, G.; Panou, A. First Episode of Shellfish Contamination by Palytoxin-like Compounds from *Ostreopsis* Species (Aegean Sea, Greece). *Toxicon* **2008**, *51*, 418–427. [CrossRef]
10. Amzil, Z.; Sibat, M.; Chomérat, N.; Grossel, H.; Marco-Miralles, F.; Lemée, R.; Nézan, E.; Séchet, V. Ovatoxin-a and Palytoxin Accumulation in Seafood in Relation to *Ostreopsis* cf. *ovata* Blooms on the French Mediterranean Coast. *Mar. Drugs* **2012**, *10*, 477–496. [CrossRef]
11. Guiry, M.D.; Guiry, G.M. AlgaeBase. World-Wide Electronic Publication. Available online: <http://www.algaebase.org> (accessed on 25 May 2022).
12. Verma, A.; Hoppenrath, M.; Dorantes-Aranda, J.J.; Harwood, D.T.; Murray, S.A. Molecular and Phylogenetic Characterization of *Ostreopsis* (Dinophyceae) and the Description of a New Species, *Ostreopsis rhodesae* sp. nov., from a Subtropical Australian Lagoon. *Harmful Algae* **2016**, *60*, 116–130. [CrossRef] [PubMed]
13. Accoroni, S.; Romagnoli, T.; Penna, A.; Capellacci, S.; Ciminiello, P.; Dell’Aversano, C.; Tartaglione, L.; Abboud-Abi Saab, M.; Giussani, V.; Asnaghi, V.; et al. *Ostreopsis fattorussoi* Sp. Nov. (Dinophyceae), a New Benthic Toxic *Ostreopsis* Species from the Eastern Mediterranean Sea. *J. Phycol.* **2016**, *52*, 1064–1084. [CrossRef] [PubMed]
14. Penna, A.; Vila, M.; Fraga, S.; Giacobbe, M.G.; Andreoni, F.; Riobó, P.; Vernesi, C. Characterization of *Ostreopsis* and *Coolia* (Dinophyceae) Isolates in the Western Mediterranean Sea Based on Morphology, Toxicity and Internal Transcribed Spacer 5.8S rDNA Sequences. *J. Phycol.* **2005**, *41*, 212–225. [CrossRef]
15. Parsons, M.L.; Aligizaki, K.; Dechraoui Bottein, M.-Y.; Fraga, S.; Morton, S.L.; Penna, A.; Rhodes, L. *Gambierdiscus* and *Ostreopsis*: Reassessment of the State of Knowledge of Their Taxonomy, Geography, Ecophysiology, and Toxicology. *Harmful Algae* **2012**, *14*, 107–129. [CrossRef]
16. Chomérat, N.; Bilien, G.; Derrien, A.; Henry, K.; Ung, A.; Viallon, J.; Darius, H.T.; Mahana iti Gatti, C.; Roué, M.; Hervé, F.; et al. *Ostreopsis lenticularis* Y. Fukuyo (Dinophyceae, Gonyaulacales) from French Polynesia (South Pacific Ocean): A Revisit of Its Morphology, Molecular Phylogeny and Toxicity. *Harmful Algae* **2019**, *84*, 95–111. [CrossRef]
17. Hoppenrath, M.; Murray, S.; Chomérat, N.; Horiguchi, T. *Marine Benthic Dinoflagellates—Unveiling Their Worldwide Biodiversity* (Kleine Senckenberg-Reihe 54); E. Schweizerbart’sche Verlagbuchhandlung: Stuttgart, Germany, 2014.
18. Chomérat, N.; Bilien, G.; Viallon, J.; Hervé, F.; Réveillon, D.; Henry, K.; Zubia, M.; Vieira, C.; Ung, A.; Gatti, C.M.; et al. Taxonomy and Toxicity of a Bloom-Forming *Ostreopsis* Species (Dinophyceae, Gonyaulacales) in Tahiti Island (South Pacific Ocean): One Step Further towards Resolving the Identity of *O. siamensis*. *Harmful Algae* **2020**, *98*, 101888. [CrossRef]
19. Nguyen-Ngoc, L.; Doan-Nhu, H.; Larsen, J.; Phan-Tan, L.; Nguyen, X.; Lundholm, N.; Van Chu, T.; Huynh-Thi, D.N. Morphological and Genetic Analyses of *Ostreopsis* (Dinophyceae, Gonyaulacales, Ostreopsidaceae) Species from Vietnamese Waters with a Re-description of the Type Species, *O. siamensis*. *J. Phycol.* **2021**, *57*, 1059–1083. [CrossRef]
20. Boisnoir, A.; Bilien, G.; Lemée, R.; Chomérat, N. First Insights on the Diversity of the Genus *Ostreopsis* (Dinophyceae, Gonyaulacales) in Guadeloupe Island, with Emphasis on the Phylogenetic Position of *O. heptagona*. *Eur. J. Protistol.* **2022**, *83*, 125875. [CrossRef]
21. Sato, S.; Nishimura, T.; Uehara, K.; Sakanari, H.; Tawong, W.; Hariganeya, N.; Smith, K.; Rhodes, L.; Yasumoto, T.; Taira, Y.; et al. Phylogeography of *Ostreopsis* along West Pacific Coast, with Special Reference to a Novel Clade from Japan. *PLoS ONE* **2011**, *6*, e27983. [CrossRef]
22. Tawong, W.; Nishimura, T.; Sakanari, H.; Sato, S.; Yamaguchi, H.; Adachi, M. Distribution and Molecular Phylogeny of the Dinoflagellate Genus *Ostreopsis* in Thailand. *Harmful Algae* **2014**, *37*, 160–171. [CrossRef]
23. Chomérat, N.; Bilien, G.; Couté, A.; Quod, J.-P. Reinvestigation of *Ostreopsis mascarenensis* Quod (Dinophyceae, Gonyaulacales) from Réunion Island (SW Indian Ocean): Molecular Phylogeny and Emended Description. *Phycologia* **2020**, *59*, 140–153. [CrossRef]
24. Poli, M.; Ruiz-Olvera, P.; Nalca, A.; Ruiz, S.; Livingston, V.; Frick, O.; Dyer, D.; Schellhase, C.; Raymond, J.; Kulis, D.; et al. Toxicity and Pathophysiology of Palytoxin Congeners after Intraperitoneal and Aerosol Administration in Rats. *Toxicon* **2018**, *150*, 235–250. [CrossRef] [PubMed]
25. Moore, R.E.; Scheuer, P.J. Palytoxin: A New Marine Toxin from a Coelenterate. *Science* **1971**, *172*, 495–498. [CrossRef] [PubMed]
26. Medina-Pérez, N.I.; Dall’Osto, M.; Decesari, S.; Paglione, M.; Moyano, E.; Berdalet, E. Aerosol Toxins Emitted by Harmful Algal Blooms Susceptible to Complex Air-Sea Interactions. *Environ. Sci. Technol.* **2021**, *55*, 468–477. [CrossRef] [PubMed]

27. Ciminiello, P.; Dell’Aversano, C.; Iacovo, E.D.; Fattorusso, E.; Forino, M.; Tartaglione, L.; Benedettini, G.; Onorari, M.; Serena, F.; Battocchi, C.; et al. First Finding of *Ostreopsis cf. ovata* Toxins in Marine Aerosols. *Environ. Sci. Technol.* **2014**, *48*, 3532–3540. [[CrossRef](#)]
28. Casabianca, S.; Casabianca, A.; Riobó, P.; Franco, J.M.; Vila, M.; Penna, A. Quantification of the Toxic Dinoflagellate *Ostreopsis* spp. by QPCR Assay in Marine Aerosol. *Environ. Sci. Technol.* **2013**, *47*, 3788–3795. [[CrossRef](#)]
29. Ninčević Gladan, Ž.; Arapov, J.; Casabianca, S.; Penna, A.; Honsell, G.; Brovedani, V.; Pelin, M.; Tartaglione, L.; Sosa, S.; Dell’Aversano, C.; et al. Massive Occurrence of the Harmful Benthic Dinoflagellate *Ostreopsis cf. ovata* in the Eastern Adriatic Sea. *Toxins* **2019**, *11*, 300. [[CrossRef](#)]
30. Ciminiello, P.; Dell’Aversano, C.; Fattorusso, E.; Forino, M.; Magno, G.S.; Tartaglione, L.; Grillo, C.; Melchiorre, N. The Genoa 2005 Outbreak. Determination of Putative Palytoxin in Mediterranean *Ostreopsis ovata* by a New Liquid Chromatography Tandem Mass Spectrometry Method. *Anal. Chem.* **2006**, *78*, 6153–6159. [[CrossRef](#)]
31. Ciminiello, P.; Dell’Aversano, C.; Fattorusso, E.; Forino, M.; Tartaglione, L.; Grillo, C.; Melchiorre, N. Putative Palytoxin and Its New Analogue, Ovatoxin-a, in *Ostreopsis ovata* Collected along the Ligurian Coasts during the 2006 Toxic Outbreak. *J. Am. Soc. Mass Spectrom.* **2008**, *19*, 111–120. [[CrossRef](#)]
32. Ciminiello, P.; Dell’Aversano, C.; Dello Iacovo, E.; Fattorusso, E.; Forino, M.; Grauso, L.; Tartaglione, L.; Guerrini, F.; Pezzolesi, L.; Pistocchi, R.; et al. Isolation and Structure Elucidation of Ovatoxin-a, the Major Toxin Produced by *Ostreopsis ovata*. *J. Am. Chem. Soc.* **2012**, *134*, 1869–1875. [[CrossRef](#)]
33. Ciminiello, P.; Dell’Aversano, C.; Iacovo, E.D.; Fattorusso, E.; Forino, M.; Grauso, L.; Tartaglione, L.; Guerrini, F.; Pistocchi, R. Complex Palytoxin-like Profile of *Ostreopsis ovata*. Identification of Four New Ovatoxins by High-Resolution Liquid Chromatography/Mass Spectrometry. *Rapid Commun. Mass Spectrom.* **2010**, *24*, 2735–2744. [[CrossRef](#)] [[PubMed](#)]
34. Ciminiello, P.; Dell’Aversano, C.; Iacovo, E.D.; Fattorusso, E.; Forino, M.; Tartaglione, L.; Battocchi, C.; Crinelli, R.; Carloni, E.; Magnani, M.; et al. Unique Toxin Profile of a Mediterranean *Ostreopsis cf. ovata* Strain: HR LC-MSⁿ Characterization of Ovatoxin-f, a New Palytoxin Congener. *Chem. Res. Toxicol.* **2012**, *25*, 1243–1252. [[CrossRef](#)] [[PubMed](#)]
35. Garcia-Altares, M.; Tartaglione, L.; Dell’Aversano, C.; Carnicer, O.; de la Iglesia, P.; Forino, M.; Diogène, J.; Ciminiello, P. The Novel Ovatoxin-g and Isobaric Palytoxin (so Far Referred to as Putative Palytoxin) from *Ostreopsis cf. ovata* (NW Mediterranean Sea): Structural Insights by LC-High Resolution MS. *Anal. Bioanal. Chem.* **2015**, *407*, 1191–1204. [[CrossRef](#)] [[PubMed](#)]
36. Brissard, C.; Hervé, F.; Sibat, M.; Séchet, V.; Hess, P.; Amzil, Z.; Herrenknecht, C. Characterization of Ovatoxin-h, a New Ovotoxin Analog, and Evaluation of Chromatographic Columns for Ovotoxin Analysis and Purification. *J. Chromatogr. A* **2015**, *1388*, 87–101. [[CrossRef](#)]
37. Tartaglione, L.; Dello Iacovo, E.; Mazzeo, A.; Casabianca, S.; Ciminiello, P.; Penna, A.; Dell’Aversano, C. Variability in Toxin Profiles of the Mediterranean *Ostreopsis cf. ovata* and in Structural Features of the Produced Ovatoxins. *Environ. Sci. Technol.* **2017**, *51*, 13920–13928. [[CrossRef](#)]
38. Guerrini, F.; Pezzolesi, L.; Feller, A.; Riccardi, M.; Ciminiello, P.; Dell’Aversano, C.; Tartaglione, L.; Iacovo, E.D.; Fattorusso, E.; Forino, M.; et al. Comparative Growth and Toxin Profile of Cultured *Ostreopsis ovata* from the Tyrrhenian and Adriatic Seas. *Toxicon* **2010**, *55*, 211–220. [[CrossRef](#)]
39. Brissard, C.; Herrenknecht, C.; Séchet, V.; Hervé, F.; Pisapia, F.; Harcouet, J.; Lemée, R.; Chomérat, N.; Hess, P.; Amzil, Z. Complex Toxin Profile of French Mediterranean *Ostreopsis cf. ovata* Strains, Seafood Accumulation and Ovatoxins Prepurification. *Mar. Drugs* **2014**, *12*, 2851–2876. [[CrossRef](#)]
40. Tartaglione, L.; Mazzeo, A.; Dell’Aversano, C.; Forino, M.; Giussani, V.; Capellacci, S.; Penna, A.; Asnaghi, V.; Faimali, M.; Chiantore, M.; et al. Chemical, Molecular, and Eco-Toxicological Investigation of *Ostreopsis* sp. from Cyprus Island: Structural Insights into Four New Ovatoxins by LC-HRMS/MS. *Anal. Bioanal. Chem.* **2016**, *408*, 915–932. [[CrossRef](#)]
41. Suzuki, T.; Watanabe, R.; Uchida, H.; Matsushima, R.; Nagai, H.; Yasumoto, T.; Yoshimatsu, T.; Sato, S.; Adachi, M. LC-MS/MS Analysis of Novel Ovatoxin Isomers in Several *Ostreopsis* Strains Collected in Japan. *Harmful Algae* **2012**, *20*, 81–91. [[CrossRef](#)]
42. Uchida, H.; Taira, Y.; Yasumoto, T. Structural Elucidation of Palytoxin Analogs Produced by the Dinoflagellate *Ostreopsis ovata* IK2 Strain by Complementary Use of Positive and Negative Ion Liquid Chromatography/Quadrupole Time-of-Flight Mass Spectrometry: Structural Elucidation of Ovatoxin-a, -d, -e IK2 by LC/QTOFMS. *Rapid Commun. Mass Spectrom.* **2013**, *27*, 1999–2008. [[CrossRef](#)]
43. Usami, M.; Satake, M.; Ishida, S.; Inoue, A.; Kan, Y.; Yasumoto, T. Palytoxin Analogs from the Dinoflagellate *Ostreopsis siamensis*. *J. Am. Chem. Soc.* **1995**, *117*, 5389–5390. [[CrossRef](#)]
44. Ukena, T.; Satake, M.; Usami, M.; Oshima, Y.; Naoki, H.; Fujita, T.; Kan, Y.; Yasumoto, T. Structure Elucidation of Ostreocin D, a Palytoxin Analog Isolated from the Dinoflagellate *Ostreopsis siamensis*. *Biosci. Biotechnol. Biochem.* **2001**, *65*, 2585–2588. [[CrossRef](#)]
45. Ukena, T.; Satake, M.; Usami, M.; Oshima, Y.; Fujita, T.; Naoki, H.; Yasumoto, T. Structural Confirmation of Ostreocin-D by Application of Negative-Ion Fast-Atom Bombardment Collision-Induced Dissociation Tandem Mass Spectrometric Methods. *Rapid Commun. Mass Spectrom.* **2002**, *16*, 2387–2393. [[CrossRef](#)] [[PubMed](#)]
46. Terajima, T.; Uchida, H.; Abe, N.; Yasumoto, T. Structure Elucidation of Ostreocin-A and Ostreocin-E1, Novel Palytoxin Analogs Produced by the Dinoflagellate *Ostreopsis siamensis*, Using LC/Q-TOF MS. *Biosci. Biotech. Bioch.* **2018**, *83*, 381–390. [[CrossRef](#)] [[PubMed](#)]

47. Terajima, T.; Uchida, H.; Abe, N.; Yasumoto, T. Simple Structural Elucidation of Ostreocin-B, a New Palytoxin Congener Isolated from the Marine Dinoflagellate *Ostreopsis siamensis*, Using Complementary Positive and Negative Ion Liquid Chromatography/Quadrupole Time-of-Flight Mass Spectrometry. *Rapid Commun. Mass Spectrom.* **2018**, *32*, 1001–1007. [CrossRef]
48. Hoffmann, K.; Hermanns-Clausen, M.; Buhl, C.; Büchler, M.W.; Schemmer, P.; Mebs, D.; Kauferstein, S. A Case of Palytoxin Poisoning Due to Contact with Zoanthid Corals through a Skin Injury. *Toxicon* **2008**, *51*, 1535–1537. [CrossRef]
49. Tartaglione, L.; Dell’Aversano, C.; Mazzeo, A.; Forino, M.; Wieringa, A.; Ciminiello, P. Determination of Palytoxins in Soft Coral and Seawater from a Home Aquarium. Comparison between *Palythoa*- and *Ostreopsis*-Related Inhalatory Poisonings. *Environ. Sci. Technol.* **2016**, *50*, 1023–1030. [CrossRef]
50. Beau, N.; Allemand, D.; Molinatti, E.; Claessens, Y.-E. Intoxication à la palytoxine ou la légende de Limu-make-o’hana. *Ann. Fr. Med. Urgence* **2017**, *7*, 52–54. [CrossRef]
51. Thakur, L.K.; Jha, K.K. Palytoxin-Induced Acute Respiratory Failure. *Respir. Med. Case Rep.* **2017**, *20*, 4–6. [CrossRef]
52. Calon, T.; Sinno-Tellier, S.; de Haro, L.; Bloch, J. Exposition à la palytoxine des personnes manipulant des coraux mous d’aquarium d’eau de mer: Étude des cas rapportés au réseau des Centres antipoison de 2000 à 2017. *Toxicol. Anal. Clin.* **2019**, *31*, 64–76. [CrossRef]
53. Schulz, M.; Łoś, A.; Szabelak, A.; Strachecka, A. Inhalation Poisoning with Palytoxin from Aquarium Coral: Case Description and Safety Advice. *Arch. Ind. Hyg. Toxicol.* **2019**, *70*, 14–17. [CrossRef] [PubMed]
54. Chaudhry, N.L.; Przybek, J.; Hamilton, A.; Carley, F. Unique Case of Palytoxin-Related Keratitis. *Clin. Exp. Ophthalmol.* **2016**, *44*, 853–854. [CrossRef] [PubMed]
55. Accoroni, S.; Totti, C. The Toxic Benthic Dinoflagellates of the Genus *Ostreopsis* in Temperate Areas: A Review. *Adv. Oceanogr. Limnol.* **2016**, *7*, 1–15. [CrossRef]
56. Brescianini, C.; Grillo, C.; Melchiorre, N.; Bertolotto, R.; Ferrari, A.; Vivaldi, B.; Icardi, G.; Gramaccioni, L.; Funari, E.; Scardala, S. *Ostreopsis ovata* Algal Blooms Affecting Human Health in Genova, Italy, 2005 and 2006. *Euro Surveill.* **2006**, *11*, 3040. [CrossRef]
57. Barroso García, P.; de la Puerta, P.R.; Parrón Carreño, T.; Marín Martínez, P.; Guillén Enríquez, J. Brote con síntomas respiratorios en la provincia de Almería por una posible exposición a microalgas tóxicas. *Gac. Sanit.* **2008**, *22*, 578–584. [CrossRef]
58. Illoul, H.; Hernández, F.R.; Vila, M.; Adjas, N.; Younes, A.A.; Bournissa, M.; Koroghli, A.; Marouf, N.; Rabia, S.; Ameur, F.L.K. The Genus *Ostreopsis* along the Algerian Coastal Waters (SW Mediterranean Sea) Associated with a Human Respiratory Intoxication Episode. *Cryptog. Algol.* **2012**, *33*, 209–216. [CrossRef]
59. Penna, A.; Fraga, S.; Battocchi, C.; Casabianca, S.; Giacobbe, M.G.; Riobó, P.; Vernesi, C. A Phylogeographical Study of the Toxic Benthic Dinoflagellate Genus *Ostreopsis* Schmidt. *J. Biogeogr.* **2010**, *37*, 830–841. [CrossRef]
60. Tibiriçá, C.E.J.A.; Leite, I.P.; Batista, T.V.V.; Fernandes, L.F.; Chomérat, N.; Herve, F.; Hess, P.; Mafra, L.L. *Ostreopsis cf. ovata* Bloom in Currais, Brazil: Phylogeny, Toxin Profile and Contamination of Mussels and Marine Plastic Litter. *Toxins* **2019**, *11*, 446. [CrossRef]
61. Nascimento, S.M.; Neves, R.A.F.; De’Carli, G.A.L.; Borsato, G.T.; da Silva, R.A.F.; Melo, G.A.; de Moraes, A.M.; Cockell, T.C.; Fraga, S.; Menezes-Salgueiro, A.D.; et al. *Ostreopsis cf. ovata* (Dinophyceae) Molecular Phylogeny, Morphology, and Detection of Ovatoxins in Strains and Field Samples from Brazil. *Toxins* **2020**, *12*, 70. [CrossRef]
62. Silva, A.; Brotas, V.; Orive, E.; Neto, A. First Records of *Ostreopsis heptagona*, *O. cf. siamensis* and *O. cf. ovata*—In the Azores Archipelago, Portugal. *Harmful Algae News* **2010**, *42*, 1–2. Available online: <https://hdl.handle.net/10400.3/1200> (accessed on 10 July 2022).
63. Bennouna, A.; El Attar, J.; Abouabdellah, R.; Palma, S.; Penna, A.; Moita, M.T. First Records of *Ostreopsis cf. Siamensis* in Moroccan Atlantic Upwelling Waters. *Harmful Algae News* **2010**, *42*, 1–3. Available online: <https://hdl.handle.net/11576/2503674> (accessed on 10 July 2022).
64. David, H.; Nascimento, P.; Melo, R.; Amorim, A.; Caeiro, M.F. Bloom of *Ostreopsis cf. siamensis* in Lisbon Bay. *Harmful Algae News* **2018**, *60*, 11–12.
65. Amorim, A.; Veloso, V.; Penna, A. First Detection of *Ostreopsis cf. siamensis* in Portuguese Coastal Waters. *Harmful Algae News* **2010**, *42*, 6–7. Available online: <https://hdl.handle.net/11576/2503669> (accessed on 10 July 2022).
66. Laza-Martínez, A.; Orive, E.; Irati, M. Morphological and Genetic Characterization of Benthic Dinoflagellates of the Genera *Coolia*, *Ostreopsis* and *Prorocentrum* from South-Eastern Bay of Biscay. *Eur. J. Phycol.* **2011**, *46*, 45–65. [CrossRef]
67. David, H.; Laza-Martínez, A.; Miguel, I.; Orive, E. *Ostreopsis cf. siamensis* and *Ostreopsis cf. ovata* from the Atlantic Iberian Peninsula: Morphological and Phylogenetic Characterization. *Harmful Algae* **2013**, *30*, 44–55. [CrossRef]
68. Ramos, V.; Salvi, D.; Machado, J.; Vale, M.; Azevedo, J.; Vasconcelos, V. Culture-Independent Study of the Late-Stage of a Bloom of the Toxic Dinoflagellate *Ostreopsis cf. ovata*: Preliminary Findings Suggest Genetic Differences at the Sub-Species Level and Allow ITS2 Structure Characterization. *Toxins* **2015**, *7*, 2514–2533. [CrossRef]
69. Santos, M.; Oliveira, P.B.; Moita, M.T.; David, H.; Caeiro, M.F.; Zingone, A.; Amorim, A.; Silva, A. Occurrence of *Ostreopsis* in Two Temperate Coastal Bays (SW Iberia): Insights from the Plankton. *Harmful Algae* **2019**, *86*, 20–36. [CrossRef]
70. Seoane, S.; Siano, R. New Limits of *Ostreopsis* Distribution in the Bay of Biscay: A First Report of *Ostreopsis* in Santander Bay, Cantabria (Northern Spain). *Harmful Algae News* **2018**, *60*, 10. Available online: <https://unesdoc.unesco.org/ark:/48223/pf0000266184> (accessed on 10 July 2022).

71. Drouet, K.; Jauzein, C.; Herviot-Heath, D.; Hariri, S.; Laza-Martinez, A.; Lecadet, C.; Plus, M.; Seoane, S.; Sourisseau, M.; Lemée, R.; et al. Current Distribution and Potential Expansion of the Harmful Benthic Dinoflagellate *Ostreopsis* cf. *Siamensis* towards the Warming Waters of the Bay of Biscay, North-East Atlantic. *Environ. Microbiol.* **2021**, *23*, 4965–4979. [[CrossRef](#)]
72. Deeds, J.R.; Schwartz, M.D. Human Risk Associated with Palytoxin Exposure. *Toxicon* **2010**, *56*, 150–162. [[CrossRef](#)]
73. Pelin, M.; Sosa, S.; Ponti, C.; Gibellini, D.; Florio, C.; Tubaro, A. Pro-Inflammatory Effects of Palytoxin on Skin Keratinocytes and Indirect Modulation of Inflammatory Cells. *Toxicon* **2018**, *149*, 97. [[CrossRef](#)]
74. Mangialajo, L.; Ganzin, N.; Accoroni, S.; Asnaghi, V.; Blanfuné, A.; Cabrini, M.; Cattaneo-Vietti, R.; Chavanon, F.; Chiantore, M.; Cohu, S.; et al. Trends in *Ostreopsis* Proliferation along the Northern Mediterranean Coasts. *Toxicon* **2011**, *57*, 408–420. [[CrossRef](#)]
75. Pistocchi, R.; Pezzolesi, L.; Guerrini, F.; Vanucci, S.; Dell’Aversano, C.; Fattorusso, E. A Review on the Effects of Environmental Conditions on Growth and Toxin Production of *Ostreopsis ovata*. *Toxicon* **2011**, *57*, 421–428. [[CrossRef](#)] [[PubMed](#)]
76. Drouet, K.; Jauzein, C.; Gasparini, S.; Pavaux, A.-S.; Berdalet, E.; Marro, S.; Davenet-Sbirruzuoli, V.; Siano, R.; Lemée, R. The Benthic Toxic Dinoflagellate *Ostreopsis* cf. *ovata* in the NW Mediterranean Sea: Relationship between Sea Surface Temperature and Bloom Phenology. *Harmful Algae* **2022**, *112*, 102184. [[CrossRef](#)] [[PubMed](#)]
77. David, H.; Ganzedo, U.; Laza-Martínez, A.; Orive, E. Relationships between the Presence of *Ostreopsis* (Dinophyceae) in the Atlantic Coast of the Iberian Peninsula and Sea-Surface Temperature. *Cryptog. Algol.* **2012**, *33*, 199–207. [[CrossRef](#)]
78. Gémin, M.-P.; Réveillon, D.; Hervé, F.; Pavaux, A.-S.; Tharaud, M.; Séchet, V.; Bertrand, S.; Lemée, R.; Amzil, Z. Toxin Content of *Ostreopsis* cf. *ovata* Depends on Bloom Phases, Depth and Macroalgal Substrate in the NW Mediterranean Sea. *Harmful Algae* **2020**, *92*, 101727. [[CrossRef](#)]
79. Nascimento, S.M.; Corrêa, E.V.; Menezes, M.; Varela, D.; Paredes, J.; Morris, S. Growth and Toxin Profile of *Ostreopsis* cf. *ovata* (Dinophyta) from Rio de Janeiro, Brazil. *Harmful Algae* **2012**, *13*, 1–9. [[CrossRef](#)]
80. Ciminiello, P.; Dell’Aversano, C.; Iacovo, E.D.; Fattorusso, E.; Forino, M.; Tartaglione, L.; Yasumoto, T.; Battocchi, C.; Giacobbe, M.; Amorim, A.; et al. Investigation of Toxin Profile of Mediterranean and Atlantic Strains of *Ostreopsis* cf. *siamensis* (Dinophyceae) by Liquid Chromatography-High Resolution Mass Spectrometry. *Harmful Algae* **2013**, *23*, 19–27. [[CrossRef](#)]
81. Cagide, E.; Louzao, M.C.; Espiña, B.; Vieytes, M.R.; Jaen, D.; Maman, L.; Yasumoto, T.; Botana, L.M. Production of Functionally Active Palytoxin-like Compounds by Mediterranean *Ostreopsis* cf. *siamensis*. *Cell Physiol. Biochem.* **2009**, *23*, 431–440. [[CrossRef](#)]
82. Drouet, K. Impact de la température sur la Biogéographie et la Phénologie des Dinoflagellés Benthiques Toxiques du Genre *Ostreopsis* en Méditerranée et en Atlantique. Ph.D. Thesis, Sorbonne University, Paris, France, 2021.
83. Verma, A.; Hoppenrath, M.; Harwood, T.; Brett, S.; Rhodes, L.; Murray, S. Molecular Phylogeny, Morphology and Toxigenicity of *Ostreopsis* cf. *siamensis* (Dinophyceae) from Temperate South-East Australia. *Phycol. Res.* **2016**, *64*, 146–159. [[CrossRef](#)]
84. Pavaux, A.-S.; Berdalet, E.; Lemée, R. Chemical Ecology of the Benthic Dinoflagellate Genus *Ostreopsis*: Review of Progress and Future Directions. *Front. Mar. Sci.* **2020**, *7*, 498. [[CrossRef](#)]
85. Chomérat, N.; iti Gatti, C.M.; Nézan, E.; Chinain, M. Studies on the Benthic Genus *Sinophysis* (Dinophysales, Dinophyceae) II. *S. canaliculata* from Rapa Island (French Polynesia). *Phycologia* **2017**, *56*, 193–203. [[CrossRef](#)]
86. Lazure, P.; Dumas, F. An External–Internal Mode Coupling for a 3D Hydrodynamical Model for Applications at Regional Scale (MARS). *Adv. Water Resour.* **2008**, *31*, 233–250. [[CrossRef](#)]
87. Guillard, R.R.L.; Hargraves, P.E. *Stichochrysis immobilis* is a Diatom, not a chrysophyte. *Phycologia* **1993**, *32*, 234–236. [[CrossRef](#)]
88. Nunn, G.B.; Theisen, B.F.; Christensen, B.; Arctander, P. Simplicity-Correlated Size Growth of the Nuclear 28S Ribosomal RNA D3 Expansion Segment in the Crustacean Order Isopoda. *J. Mol. Evol.* **1996**, *42*, 211–223. [[CrossRef](#)]
89. Nézan, E.; Siano, R.; Boulben, S.; Six, C.; Bilien, G.; Chèze, K.; Duval, A.; Le Panse, S.; Quéré, J.; Chomérat, N. Genetic Diversity of the Harmful Family Kareniaeae (Gymnodiniales, Dinophyceae) in France, with the Description of *Karlodinium gentienii* sp. Nov.: A New Potentially Toxic Dinoflagellate. *Harmful Algae* **2014**, *40*, 75–91. [[CrossRef](#)]
90. Katoh, K.; Rozewicki, J.; Yamada, K.D. MAFFT Online Service: Multiple Sequence Alignment, Interactive Sequence Choice and Visualization. *Brief. Bioinform.* **2019**, *20*, 1160–1166. [[CrossRef](#)]
91. Guindon, S.; Dufayard, J.-F.; Lefort, V.; Anisimova, M.; Hordijk, W.; Gascuel, O. New Algorithms and Methods to Estimate Maximum-Likelihood Phylogenies: Assessing the Performance of PhyML 3.0. *Syst. Biol.* **2010**, *59*, 307–321. [[CrossRef](#)]
92. Ronquist, F.; Huelsenbeck, J.P. MrBayes 3: Bayesian Phylogenetic Inference under Mixed Models. *Bioinformatics* **2003**, *19*, 1572–1574. [[CrossRef](#)]
93. Uemura, D.; Hirata, Y. Studies on Palytoxins. *Tetrahedron* **1985**, *41*, 1007–1017. [[CrossRef](#)]
94. Ciminiello, P.; Dell’Aversano, C.; Dello Iacovo, E.; Fattorusso, E.; Forino, M.; Grauso, L.; Tartaglione, L.; Florio, C.; Lorenzon, P.; De Bortoli, M.; et al. Stereostructure and Biological Activity of 42-Hydroxy-Palytoxin: A New Palytoxin Analogue from Hawaiian *Palythoa* Subspecies. *Chem. Res. Toxicol.* **2009**, *22*, 1851–1859. [[CrossRef](#)] [[PubMed](#)]
95. Kerbrat, A.S.; Amzil, Z.; Pawlowiez, R.; Golubic, S.; Sibat, M.; Darius, H.T.; Chinain, M.; Laurent, D. First Evidence of Palytoxin and 42-Hydroxy-Palytoxin in the Marine Cyanobacterium *Trichodesmium*. *Marine Drugs* **2011**, *9*, 543–560. [[CrossRef](#)] [[PubMed](#)]
96. Lenoir, S.; Ten-Hage, L.; Turquet, J.; Quod, J.-P.; Bernard, C.; Hennion, M.-C. First Evidence of Palytoxin Analogues from an *Ostreopsis Mascarenensis* (Dinophyceae) Benthic Bloom in Southwestern Indian Ocean. *J. Phycol.* **2004**, *40*, 1042–1051. [[CrossRef](#)]
97. Rossi, R.; Castellano, V.; Scalco, E.; Serpe, L.; Zingone, A.; Soprano, V. New Palytoxin-like Molecules in Mediterranean *Ostreopsis* cf. *ovata* (Dinoflagellates) and in *Palythoa Tuberculosa* Detected by Liquid Chromatography-Electrospray Ionization Time-of-Flight Mass Spectrometry. *Toxicon* **2010**, *56*, 1381–1387. [[CrossRef](#)]